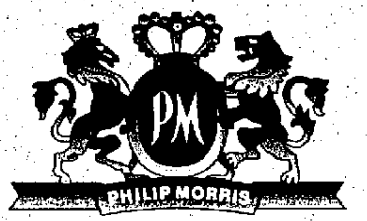

Fifth
Philip Morris USA Symposium
on
Fundamental Science

Philip Morris USA
Richmond, Virginia
October 28-30, 2003

Welcome!

It is once again my great pleasure to welcome you to our latest (and 5th) Philip Morris USA Symposium on Fundamental Science! It is both an honor and a treat to serve as your host, whether you come from far or from near. As I write this message, I warmly anticipate seeing so many friends and colleagues and hearing great science.

The organizing committee and I are very pleased to offer you this opportunity to participate in what surely will be an exciting and informative symposium. As in the past, the enclosed abstracts provide an elegant appetizer for a diverse and thoughtful series of presentations. The emphasis of this year's symposium will be on "reduced exposure cigarette products." As indicated in the enclosed abstracts, the papers and posters will cover a larger area of science than in any of our previous symposia. We especially welcome this diversity of topics and presenters.

As in the past, the symposium's underlying theme is fundamental science. All the presentations and posters should be related to our basic research and fundamental understandings. **Please do not disclose and discuss any matter that could be proprietary in nature**. One objective of the symposium is information sharing. We encourage full discussions among the participants. **However, outside speakers and attendees acknowledge that Philip Morris' confidential and proprietary information may be presented during the course of the symposium. Outside speakers and attendees agree to hold in confidence and refrain from using any Philip Morris technical or business information presented during the symposium which is not publicly available.**

In addition, much of the work is "work in progress." Hence, the conclusions, in many cases, are preliminary; indeed, some of the data presented may be preliminary. It is in these contexts that we encourage all of you to participate in these discussions of state-of-the-art science and emerging science and technology. We hope that your time here will be professionally useful and personally fulfilling. I look forward to speaking with each of you personally. Again, my warmest welcome to you.

On behalf of the organizing committee,

Mohammad Hajaligol

Organizing Committee

Geoffrey Chan

Jay Fournier

Diane Gee

Mohammad Hajaligol

Alec Hayes

Betty Mitchell

Hans Roethig

Jeffery Seeman

Fifth Philip Morris USA Symposium on Fundamental Science

Jefferson Hotel
Richmond, Virginia
October 28-30, 2003

Tuesday, October 28, 2003		
7:30	**Breakfast**	
Session 1: Relationships between Disease, Biological Endpoints and Chemistry of Tobacco Smoke		
Chair: Geoffrey Chan		
8:15	Special Welcome and Opening Remark	**Jack Nelson**, President, Operations & Technology
8:30	Introduction and Agenda Review	**Mohammad Hajaligol**
8:45	Smoking Related Diseases, Disease Models, and Mechanisms	**Klaus von Holt**
9:05	Identification of Cell-Stressing Smoke Constituents	**Thomas Mueller**
9:25	Mechanistic Studies to Investigate the Effect of AMP in Cigarette Paper	**E. Roemer**, B.P. Mueller, T.J. Meisgen, and E. Anskeit
9:45	Biomarkers to Assess Potential Harm in Adult Cigarette Smokers and Non-smokers	**Barbara K. Zedler**
10:05	**Break**	
Chair: Jay Fournier		
10:30	Oxidative Stress and Inflammation	**Mathias Schorp**
10:50	Reactive Oxygen Species (ROS) Related to Exposure to Cigarette Smoke: Overview on ROS Mechanistic Processes and Biosensing Approaches	**G.D. Griffin**, F. Yan, R. Jagannathan, C. Brooks, T. Vo-Dinh, S. E. Plunkett, K. H. Shafer, and W. Reininghaus
11:10	Does Puffing Profile Determine Exposure to Cigarette Smoke Constituents	Candace Adams, Hans Roethig, Qiwei Liang, Jin Yan and **Mohamadi Sarkar**
11:30	Clinical Risk Evaluation of Potential-Reduced Exposure Products	**Martin Unverdorben**
11:50	**Lunch**	

Fifth Philip Morris USA Symposium on Fundamental Science

Jefferson Hotel
Richmond, Virginia
October 28-30, 2003

Tuesday, October 28, 2003		
Session 2: Role of Tobacco and Tobacco Related Materials, Including Chars, in Modifying Smoke Chemistry		
Chair: Candace Adams		
1:00	A Review of Important Morphological Findings of Tobacco, Tobacco Components, and the Cigarette Coal	**Vicki L. Baliga**, Ramesh K. Sharma, Michael E. Thurston, Donald E. Miser, W. Geoffrey Chan, and Mohammad R. Hajaligol
1:20	Effect of Metal Doping of either Cellulose or Tobacco on Charring and Reactive Intermediates Detected by Laser Pyrolysis MBMS	**Andrew M. Herring**, J. Thomas McKinnon, Joshua Lee, Bryan D. McClosky, Ryan A. Pavelka and Matthew Kirchner
1:40	Reduction of BAP Yields from Cellulose by the Addition of Pd Salts	**Thomas E. McGrath**, Gail Yoss, Jan B. Wooten and W. Geoffrey Chan
2:00	XPS Study of Cellulose and Tobacco Char	**W. Z. Zhu**, Thomas E. McGrath, and W. Geoffrey Chan
2:15	Heterogeneous Expression and Directed Evolution of UDP-glucose Dehydrogenase	Xuan Guo, W. Geoffrey Chan, and **Rachel Chen**
2:30	**Break**	
Chair: Bill Gardner		
2:50	Chemistry of Cigarette Burning and Smoke Formation	**Peishi Chen**
3:10	Smoke Chemistry of a Cigarette that is Extinguished and Relit	**Peter Lipowicz**, San Li, Ila Skinner, and Milton Parrish
3:30	Effects of Smoking Parameters on Smoke Yields and Their Prediction for EHCSS	**Zuyin "Frank" Yang**, John Hearn, and Sue Wrenn
3:50	An Experimental and Modeling Study to Predict Products Yields During Puffing	**M.S. Saidi**, M.R. Hajaligol, F. Rasouli, P.J. Lipowicz, K.H. Shafer and M.S. Rostami
4:10	Sub-model Development for Tobacco Char Oxidation and CO2 Gasification	**Hong-Shig Shim** and Adel Sarofim
4:30	**Poster Session 1 (Chair: Weijun Zhang)**	
6:00	**Reception**	

Fifth Philip Morris USA Symposium on Fundamental Science

Jefferson Hotel
Richmond, Virginia
October 28-30, 2003

Wednesday, October 29, 2003		
7:30	**Breakfast**	
Session 3: Free Radicals: Formation and Properties in Smoke		
Chair: Newton Kalengamaliro		
8:15	Opening Remarks	**Hector Alonso**, Vice President, Product Development & Technology
8:30	Subjective Properties of Cigarette Smoke	**Gerd Kobal**
9:05	A Predictive Model of Concentration of Persistent Radicals in Tobacco Smoke	**Zofia Maskos**, Lavrent Khachatryan, Rafael Cueto, William A. Pryor, and Barry Dellinger
9:25	Fluorometric Approach for quantitation of free radicals in cigarette smoke	**Dejian Huang** and Boxin Ou
9:45	Formation of Radicals by Oxygen Chemisorption in Charred Burley Tobacco	Ji-Wen Feng and **Jan B. Wooten**
10:05	In-Situ High Temperature EPR Investigations of the Charring and Char Oxidation of Cellulose, Cellulose/Na2CO3 Mixtures and Tobacco	Shaokuan Zheng, Ji-Wen Feng, and **Gary E. Maciel**
10:25	**Break**	
Session 4: Formation, Characterization, and Reactivity of the Gas/Vapor Phase of Smoke		
Chair: Susan Plunkett		
10:40	13CO and 13CO C-13 NMR Imaging Gas Phase Measurement in the presence/Absence of a Nanophase Transition Metal Oxide Catalyst	**David E Axelson** and Firooz Rasouli
11:00	Mechanism of Formation of Gas-Phase and Volatile Phase Products from the Pyrolysis of Glycerin and Glucose using C-13 Isotopic Labeling	**John B. Paine III**, Yezdi Pithawalla, John D. Naworal, and Charles E. Thomas, Jr.
11:20	Formaldehyde Formation from Mainstream Smoke Gas Phase Aging	**San Li**, Joseph L. Banyasz and Ken H. Shafer
11:35	Multivariate Interpolation Scheme for the Functional-Group Biomass Pyrolysis Model	Eric Rubenstein, **Marek Wójtowicz**, Elizabeth Florczak and Michael Serio
11:55	Quad Quantum Cascade Laser Spectrometer fro Simultaneous Analysis of Mainstream and Sidestream Cigarette Smoke	**Randall Baren**, Milton Parrish, Ken Shafer, Charles Harward, Q. Shi, D. Nelson, B. McManus, and M. Zahniser
12:10	**Lunch**	

Fifth Philip Morris USA Symposium on Fundamental Science

Jefferson Hotel
Richmond, Virginia
October 28-30, 2003

Wednesday, October 29, 2003		
Session 5: Formation, Characterization, and Reactivity of the Particular Phase of Smoke		
Chair: Ila Skinner		
1:10	Development of GC-Combustion-Isotope Ratio Mass Spectrometry for Analysis of PAH in Mainstream Smoke: Investigation of Precursor-Product Relationships	**Phillip F. Britt**, A. C. Buchanan III, Roger A. Jenkins, Deon Bennett, and J. Todd Skeen
1:30	Maillard Chemistry in Char Maturation: Comparison of Different Amino Acids	**Mark Nimlos**, Thomas Sherow, Karl Andreason, Mike Looker, Bob Evans, and Luc Moens
1:50	Phenolic Compound Formation from Tobacco and Tobacco Components	**Thomas E. McGrath**, Raquel M. Olegario, Gayle M. Powers and W. Geoffrey Chan
2:10	Reduction of HQ and Catechol by Catalyst and Ammonia	**Eun-Jae Shin**, W. Geoffrey Chan, Firooz Rasouli and Mohammad R. Hajaligol
2:30	Characterization of the Particle Size Distribution of Mainstream Cigarette Smoke	**David Kane** and Peter Lipowicz
2:50	**Break**	
Chair: Vicki Baliga		
3:20	Identification of Nitro-PAH in Tobacco Smoke using Electron Monochromator Mass Spectrometry	**John Dane,** Kent J. Voorhees, Crystal Havey, Christy Abbas-Hawkes, and Robert B. Cody
3:30	Vapor Pressures of Tobacco Tar Related Materials	**Vahur Oja** and Mohammad Hajaligol
3:50	Pyrolysis and Oxidation of Biomass with Nanoparticle Iron Oxide	**Ping Li,** Firooz Rasouli, and Mohammad R. Hajaligol
4:10	Investigation of Adsorbents for the Selective Filtration of Gas-phase Components in the Cigarette Smoke	**Mark S. Zhuang,** Diane Gee, Jose Nepomuceno, and George Karles
4:30	**Poster Session 2 (Chair: Zhaohua Luan)**	
6:30	**Cocktail and Banquet**	

Fifth Philip Morris USA Symposium on Fundamental Science

Jefferson Hotel
Richmond, Virginia
October 28-30, 2003

Thursday, October 30, 2003		
7:30	**Breakfast**	
Session 6: Role of Adsorbents and Catalysts in Modifying Smoke Chemistry		
Chair: Yezdi Pithawalla		
8:15	Opening Remarks	**Rick Solana**, Vice President, Worldwide Scientific Affairs
8:30	Sequential Oxidation of Transition Metal and Nobel Metal Cluster	**Purusottam Jena**
8:50	Catalysis Study from First Principles: CO Oxidation on Au/TiO2, CO and NO reaction on Pd clusters	Xueyuan Wu, Annabella Selloni, Michele Lazzeri, Joshua Whitney, Yiming Zhang, and **Saroj K. Nayak**
9:10	Metal Oxide Catalysis of CO/NO to CO2/N2: Fe_mO_n and Cu_mO_n Nanoparticles	**Elliot R. Bernstein**, D. N. Shin, and Y. Matsuda
9:30	Gold Nanoparticle Catalysts for Low Temperature CO Oxidation	Khaled Saoud, **M. Samy El-Shall,** and Sarojini Deevi
9:50	Synthesis of Nanoscale Au/Fe_2O_3 Catalysts for CO Oxidation by Deposition-Precipitation Technique	Mikhail Khoudiakov, Mool C. Gupta, and **Sarojini Deevi**
10:05	**Break**	
Chair: Shalva Gedevanishvili		
10:20	Evaluation of a manganese ferrite based mixed oxide system as CO oxidation catalyst	**S. PalDey**, S. Gedevanishvili, and F. Rasouli
10:35	Evaluation of Low Temperature Au/TiO_2 catalyst for Removal of CO from Cigarette Smoke	**Yezdi B. Pithawalla** and Sarojini Deevi
10:50	Feasibility of NO Reduction via CO Oxidation: A Model study for Iron-oxide Particles	**B. V. Reddy**, F. Rasouli and S. N. Khanna
11:05	Infrared Spectroscopy of CO Oxidation by a Cobalt-Based Oxide Catalyst	**Piers Newbery**, John B. Paine, Benjamin A. Weinstock, Matthew J. Pollard, Husheng Yang and Peter R. Griffiths
11:25	SCF-Assisted Microencapsulation Studies	**Mark A. McHugh**, Zhihao Shen, Dan Li, and Georgios D. Karles
11:45	Concluding Remarks	**Mohammad Hajaligol**
12:00	**Lunch**	
Meeting Adjourn		

Oral Presentations

Smoking Related Diseases, Disease Models, and Mechanisms

Klaus von Holt
PHILIP MORRIS Research Laboratories GmbH, Cologne, Germany

Cigarette smoking is a major risk factor for cancer, cardiovascular disease, and chronic obstructive pulmonary disease. The effects of smoking on these diseases are dose-dependent and can be observed across different countries and cultures. Among the ever increasing number of constituents that have been identified in cigarette smoke, representatives for different classes of constituents are measured routinely. These constituents may have various types of toxic effects, such as irritation, cytotoxicity, mutagenicity, and carcinogenicity. Human exposure data can link chemical analysis data to potential harm for smokers. Risk assessment and harm reduction research will be facilitated by appropriate *in vitro* assays and animal models for the pathogenesis of tobacco-related diseases. These models need to have a mechanistic link to the disease and end points corresponding to human symptoms. Guiding principles for assay development are consistency among clinical, in vivo, and in vitro markers, finding common modes of action between disease areas to increase our understanding of smoking-related adverse health effects, and identifying smoke constituents with a broad spectrum of activities in various diseases to improve our input for product development.

Identification of Cell-Stressing Smoke Constituents

Thomas Mueller
PHILIP MORRIS Research Laboratories GmbH, Cologne, Germany

HYPOTHESIS – Cigarette smoke (CS) harbors a strong oxidative stress potential, which broadly impacts exposed cells. While this cell-damaging activity of CS, which is believed to be linked to the development of CS-related diseases, is strongly attributable to the water-soluble fraction of smoke, our knowledge about the *identity* and the *mechanisms* of CS-related constituents involved in this process is incomplete.

RESULTS – Using cultured murine fibroblasts (3T3 cells) exposed to aqueous extracts of CS, it is shown: (***a***) That it is mainly hydroxyl radicals produced by *Fenton/Haber-Weiss* chemistry, which induce damage to the *cell nucleus* as reflected by the formation of DNA strand breaks. This process is fueled by the superoxide anion, which is continuously produced in the presence of semiquinones and polyphenols such as catechol known to be present in CS. (***b***) In contrast to nucleic acid-damaging hydroxyl radicals, compounds highly reactive to sulfhydryl residues are obviously involved in inducing stress *signal transduction* processes leading to global changes in the gene expression pattern of exposed cells. As exemplified for the differential expression of the c-*fos* gene, used as a stress reporter gene, peroxynitrite, the reaction product of superoxide and nitric oxide, was identified as a CS-specific stress signaling compound. (***c***) In order to exert its (stress) gene-inducing effects, CS-dependent peroxynitrite requires a depleted pool of *cytosolic* thiols such as glutathione and thioredoxin, which is brought about by the presence of CS-related aldehydes, *i.e.*, acrolein, acetaldehyde, and formaldehyde.

CONCLUSIONS – Various specific CS constituents have been identified, which have been shown to affect exposed cells from the cell membrane to the nucleus. In mechanistic terms, the molecular effects reflect, at least in part, the genotoxic activity of CS as well as the pro-inflammatory activity of CS, both of which are assumed to be causally linked to the development of CS-related diseases, such as cancer, COPD, and cardiovascular disease.

Mechanistic Studies to Iinvestigate the Effect of AMP in Cigarette Paper

E. Roemer, B.P. Mueller, T.J. Meisgen, and E. Anskeit
PHILIP MORRIS Research Laboratories GmbH, Cologne, Germany

<Abstract Not Available>

AMP vs. $CaCO_3$
AMP effect (1) not related to depletion of oxygen (2) is related to NH_3

Biomarkers to Assess Potential Harm in Adult cigarette Smokers and Non-Smokers

Barbara K. Zedler
Philip Morris USA, Richmond, Virginia

<Abstract Not Available>

Pilot TES

LDL Chol
HDL Chol
Fibrinogen
(2) indicators of oxidative stress

Oxidative Stress and Inflammation

Mathias Schorp
Philip Morris International, Neuchatel, Switzerland

<Abstract Not Available>

Reactive Oxygen Species (ROS) Related to Exposure to Cigarette Smoke: Overview on ROS Mechanistic Processes and Biosensing Approaches

G. D. Griffin[1], F. Yan[1], R. Jagannathan[1], C. Brooks[1], T. Vo-Dinh[1], S. E. Plunkett[2], K. H. Shafer[2], and W. Reininghaus[3]
[1]Oak Ridge National Laboratory, Oak Ridge, Tennessee
[2]Philip Morris USA, Richmond, Virginia
[3]Philip Morris Research Laboratory GmbH, Cologne, Germany

This presentation will provide an overview of reactive oxygen species (ROS) associated with exposure to cigarette smoke. We will discuss mechanistic processes related to the occurrence of ROS in cellular systems. Increased intracellular levels of ROS such as superoxide, hydroxyl radical, or hydrogen peroxide (H_2O_2) are related to oxidative stress, which is caused by an imbalance between oxidants and antioxidants in favor of the former. Cigarette smoking can cause an acute inflammatory reaction in the lung, producing ROS and nitrogen species at high concentrations.

We will also provide an overview of various methods for monitoring important ROS such as H_2O_2, using electrochemical and optical techniques including fluorescence and chemiluminescence. The focus of our monitoring approach is to quantify hydrogen peroxide generated following solvation of mainstream cigarette smoke in aqueous media. Analytical aspects of the techniques including sensitivity, selectivity and reliability are discussed. Preliminary results obtained in our laboratory, and the implications of our approach on the measurements of extracellular and intracellular H_2O_2, are presented.

Does Puffing Profile Determine Exposure to Cigarette Smoke Constituents?

Candace Adams, Hans Roethig, Qiwei Liang, Jin Yan and **Mohamadi Sarkar**
Philip Morris USA, Richmond, Virginia

<Abstract Not Available>

puff vol
interpuff interval > most important as contributors

Clinical Risk Evaluation of Potential-Reduced Exposure Products

Martin Unverdorben
Philip Morris USA, Richmond, Virginia

The primary objective of risk evaluation is the prediction of harm to a population.

For clinical risk evaluation of potential-reduced exposure products (PREPs) Philip Morris will conduct short term and long term studies.

Parameters to be evaluated in risk evaluation trials will include clinical, chemical, morphologic, and functional tests.

Biomarkers of potential harm to be evaluated comprise body weight, blood pressure, pulse rate, white and red blood cell count, carboxyhemoglobin, high sensitive C-reactive protein, fibrinogen, von Willebrand factor, serum lipids, total bilirubin, 8-*epi*-prostaglandin $F_{2\alpha}$, CYP1A2 enzyme, and urine albumin. Other biomarkers under consideration for these studies comprise the lipoprotein-associated phospholipase A_2, interleukin IL-10, and atrial natriuretic peptide (ANP).

The ultrasonic measurement of intima-media thickness of the carotid arteries related to the severity of atherosclerosis will be considered for risk evaluation as will be functional tests such as exercise performance, endothelial venoreactivity, and diastolic dysfunction.

Eventually, a longitudinal risk evaluation trial covering an observation period of at least 15 years is under consideration. The focus would be on disease areas which have a significant health impact such as cardiovascular disease, chronic obstructive pulmonary disease, and lung cancer.

A Review of Important Morphological Findings of Tobacco, Tobacco Components, and the Cigarette Coal

Vicki L. Baliga, Ramesh K. Sharma, Michael E. Thurston[1], Donald E. Miser, W. Geoffrey Chan, and Mohammad R. Hajaligol
Philip Morris USA, Richmond, Virginia

Hypothesis: Knowledge of morphological changes in chemical components found in tobacco, in tobacco shreds, and in the cigarette coal may help to understand changes in the chemistry that occur during the cigarette smoldering process.

Results: Tobacco components that were examined included cellulose, pectin, lignin, polyphenols, tobacco shreds, and the cigarette coal during the puff and smolder burn. Avicel cellulose softens and melts between 450 and 500 °C but if potassium salts are added, no melt occurs while palladium salts have no effect on melting. Citrus pectin softens and melts between 160 to 250 °C and by 250 °C the mass is an extensive matrix of vesicles. By 550 °C, whiskers of C and Na have formed. Alkali lignin melts by 250 °C and continues to produce volatile gases and vesicles through 750 °C. Chlorogenic acid also melts by 250 °C. Tobacco shreds during pyrolysis tend to solidify and become encrusted with inorganic salts. Tobacco shreds partially oxidized in 5% O_2 in He show migration of inorganic salts to the surface similarly to that of the pyrolyzed tobacco, but the morphology of the surface salts change with temperature and time from individually raised ridges to concentric rings of ridges that outline carbon rich valleys. The cigarette coal has at least three zones: shreds under the char line, coal, and ash. The shreds under the char line show melting and pooling of cuticle in the brown and black regions as well as vesicle formation, especially during the puff burn. The morphology of the coal region during the puff ranges from shreds with minimal damage to extensive vesicle formation both on and within the cell wall matrix, to inorganic incrustation, and to partial oxidation. The smolder burn coal exhibits melting and pooling of the cuticle, crystal growth, deposition, and encrustation with some vesicle formation, and partially oxidized shreds. Ash from both puff burn and smolder burn cigarettes tend to exhibit networks of inorganic crystals. The puff burn ash contains more partially oxidized shreds than the smolder burn ash.

Conclusions: Morphologies exhibited by pyrolyzed chemical components provide insight into the morphologies one might expect in tobaccos at specific temperatures. Lignin melts over an extended temperature range while pectin and cellulose tend to degrade over a more narrow range. Chemical components with inorganic salts respond differently from that of the pure component. Tobacco is a mixture of many chemical components with organic and inorganic salts that affect the morphologies. Also, morphologies of the cigarette coal are affected by the smoldering conditions varying from puff to natural smolder.

[1]Lancaster Laboratories, Lancaster, PA

The Effect of Metal Doping of either Cellulose or Tobacco on Charring and Reactive Intermediates Detected by Llaser Pyrolysis Molecular Beam Mass Spectroscopy, LPMBMS and Chemical Trapping

Andrew M. Herring, J. Thomas McKinnon, Joshua Lee, Bryan D. McClosky, Ryan A. Pavelka and Matthew Kirchner
Department of Chemical Engineering, Colorado School of Mines
Golden, Colorado

Hypothesis: That doping biomass with metal ions can profoundly effect the charring process and any subsequent pyrolysis events and that these effects can be used to benefit the decreased production of harmful products in cigarette smoke once they are fully understood

Results

- LPMBMS of cellulose doped with 1 and 5 wt% calcium, copper, potassium, magnesium, palladium and zinc acetates and charred at 375°C for ½ h reveals profound differences between the reactive intermediates detected. Also of interest is the suppression of the m/z 252 peak, attributed to benzo-*a*-pyrene by certain metal ions.
- Similar experiments with doped samples of bright tobacco reveal similar interesting differences
- Chemical trapping of the reactive intermediates with dimethyl disulfide confirms the changes detected by LPMBMS.
- Differences in the chars were investigated by char yields, x-ray diffraction and diffuse reflectance infrared spectroscopy.

Conclusions: Metal doping of biomass can change the chemistry of charring and the products produced during pyrolysis. Control of the reactive intermediates and aromatic fragments produced by pyrolysis by metal doping will allow the control of the product slate detected in the cigarette smoke.

Reduction of Benzo[a]pyrene Yields from Cellulose by the Addition of Pd Salts

Thomas E. McGrath, Gail Yoss, Jan B. Wooten, and W. Geoffrey Chan
Philip Morris USA, Richmond, Virginia

Hypothesis: What is the mechanism by which BaP is reduced by the addition of Pd salts to cellulose? Can the observed BaP reduction be correlated to low temperature char yields? Do different Pd salts behave similarly?

Key Results:

- Observed reduction in BaP for cellulose loaded with Pd salts: [91%] Na_2PdCl_4 ~ K_2PdCl_4 > [70%] PdOAc > [47%] $(NH_4)_2PdCl_4$ > [32%] $PdCl_2$. Pyrolysis experiments carried out in He for 10 min at 600 °C, heating rate of 600 °C/min.

- Low temperature chars have been obtained for the following salts on cellulose: NaCl, $PdCl_2$, $(NH_4)_2PdCl_4$, PdOAc, Na_2PdCl_4, and K_2PdCl_4 between 300 and 600 °C in 50 °C increments and levoglucosan yields and weight loss data have been determined. The char samples have been characterized by EA, NMR, and XPS analysis.

- Both PdOAc and Na_2PdCl_4 give large reductions in the yield of BaP, yet one yield's less char and the other more char compared to a cellulose control.

- PdOAc appears to reduce BaP yields by acting as a *dehydrogenation/gasification* catalyst during the decomposition of cellulose.

- The reduction of BaP by Na_2PdCl_4 does not appear to be the same as with PdOAc. It is hypothesized that the observed PAH reduction mechanism proceeds via a *condensation/dehydrogenation* of the residual solid.

- The effect of heating rate on BaP yields from cellulose loaded with PdOAc was found to be significant. We observed only a slight reduction in BaP under a slow heating rate of 30 °C/min. Contrary to this, Na_2PdCl_4 reduces BaP yields under both slow and fast (600 °C/min) heating rates.

Conclusions: Pd salts on cellulose reduce BaP yields. The observed reduction in the yield of BaP when PdOAc is added to cellulose can be correlated to a reduction in the amount of precursor char formed. Na_2PdCl_4 appears to reduce BaP yields by forming a more thermally stable/cross-linked char.

Conclusions Regarding the Product: A fundamental understanding of the mechanism by which the presence of Pd reduces BaP yields from cellulose may lead to a potential substitute being found for use in a lit end cigarette.

X-Ray Photoelectron Spectroscopy Study of Cellulose and Tobacco Char

W. Z. Zhu, Thomas E. McGrath, and W. Geoffrey Chan
Philip Morris USA, Richmond, Virginia

Hypothesis: X-ray photoelectron spectroscopy (XPS) is a unique and powerful surface analytical technique in revealing the structural evolution of biomass and tobacco chars as a function of pyrolysis temperature, since the binding energy of photoelectron of one particular atom is sensitive to its valence state and bonding environment as well. Additional understanding in terms of behavior of metal ions in cellulose pyrolysis, variation of composition and chemical structure of tobacco char can be achieved using this apparatus.

Results:

1. For PdOAc-loaded cellulose: As indicated by the evolution of Pd 3d profile with pyrolysis temperature, Pd particles consist primarily of Pd^{2+} and Pd^{0} states with the bulk of particles being Pd^{2+} for the unpyrolyzed material. Vast majority of the Pd^{2+} particles transform to Pd^{0} as a result of pyrolysis and the overall Pd concentration rises significantly. C 1s spectra shows that cellulose structure remains chiefly intact until 300°C during pyrolysis, at which peak characteristic of aliphatic carbon chains develops. This clearly demonstrates the decomposition of cellulose matrix and formation of carbon single bonds at this temperature.
2. For KOAc-loaded cellulose: The potassium ions are hardly detectable from the K2p spectrum for the unpyrolyzed material, presumably due to its initial low concentration and permeation into the matrix. With an increase in pyrolysis temperature, the potassium concentration rises as indicated by the strengthening intensity of K2p peak. Binding energy of C 1s peak is typical of cellulose structure for the room temperature sample. The C 1s spectrum at 300°C is suggestive of combined contributions of cellulose structure and aliphatic carbons, beyond that temperature; the cellulose structure completely collapses and is replaced by simple carbon-carbon chains. It appears the incorporation of potassium results in the earlier decomposition of cellulose during pyrolysis as compared to the palladium.
3. For Bright tobacco: The survey scan spectra at differing pyrolysis temperatures unequivocally point to the increasing concentration of inorganic species with an increase in pyrolysis temperature as determined from both photoelectron and auger electron peaks. The evolution of C1s shows the monotonic rise in the extent of aromaticity of char as the pyrolysis temperature is successively raised. The concentration of oxygen is increased with pyrolysis temperature as confirmed by both compositional analysis and rising peak intensity of the O1s peak.

Conclusions: The differing states and concentrations of Pd and K particles in cellulose matrix during pyrolysis are distinctly disclosed by analyzing their respective characteristic spectra. The influence of addition of metal ions on the decomposition behavior of cellulose can be uncovered by monitoring the evolution of C1s spectra with pyrolysis temperature.

Heterologous Expression and Directed Evolution of UDP-Glucose Dehydrogenase

Xuan Guo[1], Geoffrey Chan[2] and **Rachel Chen**[1]
[1]Department of Chemical Engineering, Virginia Commonwealth University, Richmond, Virginia
[2] Philip Morris USA, Richmond, Virginia

Polycyclic aromatic hydrocarbons (PAH) have been known produced from pyrolysis and combustion of a wide range of organic materials, such as tobacco cellulose. Since some of PAH are carcinogenic, combustion of tobacco cellulose may pose risk to public health. It is hypothesized that by transforming cellulose to its more oxidized form as polyglucuronic acid will reduce production of PAH.

A cost efficient biocatalyst system will be developed to address this issue in a regio-specific manner without jeopardizing desired property of tobacco cellulose. A gene encoding the target enzyme, UDP-glucose dehydrogenase, will be identified, cloned and expressed in *Escherichia coli* system. A large library of enzyme variants will be generated through directed evolution of the specific gene to achieve higher enzyme activity, to accept insoluble cellulose as substrate, and tolerate potential inhibition of tobacco materials. Successful expression of the enzyme in a suitable host is a prerequisite to directed evolution effort.

RkpK gene isolated from *Sinorhizobium meliloti* was cloned into expression vectors for *E. coli*. Expression of the gene was evaluated using promoters with different strength. Results indicated that weak araBAD promoter gave low expression level even through in soluble form, whereas strong T7 promoter system yielded very high expression level as analyzed by SDS-PAGE gel, however, the enzyme activity didn't match the expression level due to formation of insoluble inclusion body. The T7 system was further tuned by decreasing temperature, using minimal medium, inducing at different growth phase with various concentrations of inducer. Although functional expression was improved through the above approaches, more strategies were carried out to enhance solubility of overexpressed protein, thereby the in vivo activities. One strategy being investigated is to use low-copy number T7 expression vector, which allows us to take advantage of strong transcription rate of T7 system and adjusting folding kinetics to minimize or prevent protein aggregation. Another strategy in use is to fuse the target gene with a highly soluble protein such as maltose binding protein. Work is also in progress in directed evolution of the enzyme with several screening method being evaluated.

Chemistry of Cigarette Burning and Smoke Formation

Peishi Chen
Philip Morris USA, Richmond, Virginia

Hypothesis: Cigarette-burning and the smoke-formation processes and smoke composition are important topics for understanding cigarette performance.

Results This paper proposes the active components of Bright, Burley, and Oriental tobaccos and a basic chemistry model of the cigarette burning processes. Previous knowledge of the cigarette burning processes and smoke formation helped to establish parameters in deriving the basic chemistry equations.

Conclusions: The proposed chemistry explains the mechanisms of the cigarette burning during puffing and interpuff smoldering, and predicts the deliveries of some smoke components for cigarettes made from Bright, Burley, and Oriental tobaccos. Based on the proposed chemistry, the effect of ventilation on smoke component deliveries is discussed and the reaction heat of the puffing process is estimated.

Smoke Chemistry of a Cigarette that Is Extinguished and Relit

Peter Lipowicz, San Li, Ila Skinner, and Milton Parrish
Philip Morris USA, Richmond, Virginia

Hypothesis: Relighting a cigarette has an effect on smoke chemistry.

Results: This study provides a limited characterization of the smoke chemistry of a cigarette that has been extinguished and then relit. Cigarettes with reduced ignition propensity on standardized tests such as the NIST 10 layer filter paper test also exhibit an increased tendency to extinguish during free smolder. Such cigarettes are likely to show an increased tendency to extinguish when smoked and thus be subject to relighting. The smoke chemistry of relighting has not been explored previously. It is known that the lighting puff of a cigarette is different from subsequent puffs, characterized by lower yields of most smoke constituents, but an increase in some, such as formaldehyde. Therefore we expect that relighting also will have an effect on smoke chemistry. Smoke chemistry of a University of Kentucky 2R4F cigarette was measured using three methods: Single Puff GC/MS PAH Analysis, Puff-by-Puff FTIR Gas Phase Analysis, and Single Puff GC/MS Whole Smoke Analysis. A relit fourth puff on a 2R4F cigarette shows statistically significant decreases in smoke yields for 59 of 62 smoke constituents measured. Yield reductions were typically on the order of 25% to 75% and generally in line with the observed TPM reduction. Formaldehyde was the only constituent on the PM USA PI List that increased (55%) in the relit puff. This increase was expected because the lighting puff is elevated in formaldehyde. The puff after the relighting puff shows equivalent reductions compared to Controls for seven of eight constituents tested. This is likely caused by a significant perturbation to the smoldering of the cigarette that is not rectified in the time between puffs.

Effect of Smoking Parameters on Smoke Yields and Their Prediction for EHCSS

Zuyin "Frank" Yang, John Hearn, and Sue Wrenn
Philip Morris USA, Richmond, Virginia

Hypothesis: The aim of this study was to investigate effects of various smoke regimes on smoke TPM, tar, and nicotine yields for an Electrically Heated Cigarette Smoking System (EHCSS) and develop a model capable of predicting them under the conditions outside of those tested.

Results: A series of experiments were carried out on a five-port KC smoking machine according to a mixed 2 and 3 level experimental design (2 x 2 x 3 x 3) to investigate effects of various smoking parameters (types of puffing profile, puffing volume, puffing duration, and puffing frequency) on smoke TPM, tar, and nicotine deliveries for an EHCSS, a potentially reduced exposure product. The statistical analysis of the results showed that puffing profile, duration, frequency and volume all had significant impact on TPM, tar and nicotine yield ($p < 0.05$) while impact of quadratic terms and cross product terms accounting for interactions of these parameters on smoke product yields is insignificant ($p > 0.05$). The effects of those parameters were also ordered through Pareto charts according to their share of contribution to smoke product yields: for TPM, frequency, duration, volume, and profile were ranked first, second, third and fourth, respectively. For tar, the ranking was the same as for TPM. In contrast, for nicotine, duration, volume, frequency and profile were ranked first, second, third and fourth, respectively.

Relationships among smoke product yields and smoking parameters were determined through multivariate nonlinear regressions of both categorical and numeric variables, producing three nonlinear equations, each with four linear terms and two quadratic terms and high Pearson's correlation coefficients ($R^2 = 0.96$ for TPM, $R^2 = 0.95$ for tar, and $R^2 = 0.94$ for nicotine). The predictions of smoke product yields using these relations for a real-world smoking regime were compared with those generated in the lab under the same conditions and an excellent agreement between the predicted and measured values was achieved.

In addition, a three-layer neural network (three nodes in one hidden layer) with an S-shaped activation function was used to explore the relations among TPM, tar, and nicotine yield and smoking parameters. After only a few random tours, a global minimum was located and a nonlinear model with 24 parameters was produced, which gave an excellent agreement between the actual measured and predicted values. While excellent fitting equations with R^2 equal to 0.99 for TPM, tar and nicotine were obtained, it was difficult to interpret the physical meaning of these parameters.

Conclusion: The experimentally measured effects of puffing profile, volume, duration and frequency on smoke product yields suggest different delivery mechanisms for TPM, tar and nicotine. The nonlinear regression equations developed with the lab experimental data can be applied to predict the smoke product yields for EHCSS under real world smoking regimes.

An Experimental and Modeling Study to Predict Product Yields During Puffing

M. S. Saidi, M. R. Hajaligol, F. Rasouli, P. J. Lipowicz,
K. H. Shafer, and M. S. Rostami
Philip Morris USA, Richmond, Virginia

Hypothesis: A puff-by-puff numerical simulation of a burning cigarette is not presented in the literature yet. This paper shows some of the efforts done in this respect. The multi steps taken to achieve this goal are: puff hydrodynamics, pyrolysis and combustion modeling, formulating the heat and mass transfer coefficient between gas and tobacco shreds, and gas and aerosol transport modeling.

Results: Measuring the temperature distribution and the RTD of a puffing cigarette and combining the results with mathematical modeling of puff hydrodynamics, the agreement between the experimental and numerical results was achieved by changing the permeability of cut filler with its density and assuming negligible permeability for the burned paper and also decreasing the filter permeability properly during puffing. The boundary conditions were imposed outside the cigarette and at far distances.

The temperature-time history of a tobacco particle was derived for a puff cycle and applying the Philip Morris pyrolysis data which is the most comprehensive data available for tobacco pyrolysis, a modified pyrolysis model was derived based on a given temperature distribution in a burning cigarette and linear burn rates.

The rate of char oxidation was estimated based on the fact that coal combustion is mass transfer controlled and the local oxygen concentration and coal geometry are correlated. Since the fluid to particle heat transfer correlations derived are for geometries different than the tobacco shreds geometry, a new correlation was derived based on coupling the experimental data with numerical simulation. Using the above correlations and knowing the CO/CO2 ratio as a function of temperature, the production rate of CO and CO2 and the consumption rate of oxygen were calculated.

The transport of gaseous species in a cigarette was mathematically modeled taking into account the effect of porosity and temperature into binary gas diffusion coefficients and the amount of the mainstream smoke constituents for a puff-by-puff condition were calculated. Comparison with experiments showed good agreement.

The transport of aerosols in the cigarette was mathematically modeled based on a pore sub-model. The pore size distribution was measured and the behavior of each pore on transport of aerosol particles were modeled taking into account the Brownian, Stokes, and Saffman forces. Considering cut filler as a random distribution of pores with possible different configurations, and coupling the pore sub-model with flow distribution in the cigarette, the transport of aerosol particles in the cut filler was mathematically modeled. In a parametric study the effect of the cut filler length and porosity as well as the aerosol initial concentration and average size on the aerosol transport in the cut filler was considered and the rate of aerosol deposition and the main stream aerosol concentration as well as size distribution was calculated. Comparison with the experimental data showed good agreement.

Sub-model Development for Tobacco Char Oxidation and CO_2 Gasification

Hong-Shig Shim and Adel Sarofim
Reaction Engineering International, Salt Lake City, Utah

Hypothesis: Heterogeneous char reaction is the slowest process that occurs during typical smoking conditions and should be properly described in any modeling effort to simulate the cigarette-smoking process.

Results: REI is developing a mechanistically based sub-model for tobacco char oxidation/gasification that includes an intrinsic rate expression and a description of pore diffusion effects. A preliminary oxidation calculation shows that the diffusion controlled regime starts at about 400 °C. This calculation is consistent with Baker's data; however, the diffusion controlled regime can begin above 600 °C, depending on the orientation of individual shred. These data show that chemical kinetics must be accurately described in a combustion model for predicting this behavior. In addition to thermal decomposition and char oxidation, char gasification by CO_2 is known to be an important pathway to generate CO during smoking. An order of magnitude calculation using the n-th order power law gasification kinetics available in the literature shows that the CO contribution from char gasification can vary from <1% to 100% of the total measured CO during smoking, depending on the kinetics used. This wide variation results from the empirical nature of the power law kinetics. In addition, gas phase CO inhibition effects may not have been considered in the existing kinetic descriptions. To account for this inhibition effect during gasification, REI is developing a model to implement a Langmuir-Hinshelwood type kinetics. REI is also developing a stand-alone program to generate oxidation/gasification kinetics parameters in a closed form for Philip Morris' two-dimensional model.

Conclusions: The sub-model with mechanistic description of heterogeneous char reaction will provide the required char oxidation/gasification kinetic parameters by Philip Morris' comprehensive cigarette burning model.

Subjective Properties of Cigarette Smoke

Gerd Kobal
Philip Morris USA, Richmond, Virginia

<Abstract Not Available>

A Predictive Model of Concentration of Persistent Radicals in Tobacco Smoke

Zofia Maskos, Lavrent Khachatryan, Rafael Cueto, William A. Pryor, and Barry Dellinger
Biodynamics Institute and Department of Chemistry, Louisiana State University
Baton Rouge, Louisiana

This work was undertaken to: (1) to determine the chemical nature of the free radicals associated with the tobacco smoke generated during the pyrolysis and the oxidation of tobacco, and (2) to develop a predictive model for the temperature dependence of formation of free radicals during these processes.

The pyrolysis and oxidation of Bright tobacco or the combination of these two processes were performed over the temperature range 200-700 °C using a continuous flow-system. Both phases of the tobacco smoke - the total particulate matter (TPM) and the gas phase were collected and analyzed by electron paramagnetic resonance (EPR) spectroscopy. TPM samples were collected on the cellulose filters with the pore diameters varied from 0.1 to 5.0 μm. The unstable free radicals of the gas-phase were allowed to react with N-tert-butyl-α-phenylnitrone (PBN) resulting in the formation of a new more stable radicals, *i.e.* spin adducts.

The results of EPR experiments suggest that two kinds of free radicals are present in the collected TPM:

semiquinone radicals associated with quinone/hydroquinone-type molecular species (Q/QH_2) bound into the polymeric matrix with g-factor varied from 2.0038 to 2.0045

nitrogen-centered free radicals, g = 2.0055 to 2.0065, formed during the pyrolysis of proteins and some nitrogenous materials that is present in the tobacco leafs.

Spin-trapping solution contained alkoxy radicals (RO*) adduct with hyperfine splitting constants, a_N = 1.39 mT, a_H = 0.21 mT and g–factor 2.0064.

The concentration of free radicals varied significantly with the temperature of pyrolysis/oxidation processes and the concentration of oxygen in the reaction atmosphere. The concentration profiles versus temperature for pyrolysis and oxidation were fit to simple mathematical expressions to provide a descriptive model of the radical concentrations.

Fluorometric Approach for Quantitation of Free Radicals in Cigarette Smoke

Dejian Huang and Boxin Ou
Brunswick Laboratories, Wareham, Massachusettes

Hypothesis – Cigarette Smoke (CS) leads to oxidative stress and reactive oxygen species (ROS) including free radicals in CS are believed to be the root of the cause. Little is known about the quantity of radical oxidants in CS. Herein we propose a method in quantifying free radicals in CS by applying fluorescent probes conventionally designed to detect ROS in a biological system.

Results – We have screened the sensitivity of a host of redox sensitive fluorescent probes towards CS and identified a few probes that may be used to quantify free radical flux rates in CS. Specifically, dihydrorhodamine 123, dihydrorhodamine 6G (DHR-6G), and hydroethidine were found to be oxidized by CS and form fluorescent products. Among them, DHR-6G was the most sensitive probe towards CS. Indeed, by applying initial rate approach, we have successfully used DHR-6G in measuring radical flux rates from thermal decomposition of azo compounds such as 2,2'-Azobis(4-methoxy-2, 4-dimethyl valeronitrile) (MeOAMVN) and its analogs. By integrating a fiber optic fluorometer, an automatic smoking machine, and a gas sampler, we have constructed a system to measure oxidation rates of DHR-6G by CS in real time. If we assume radicals in CS have similar reactivity to those from thermal decomposition of azo compounds, we can then deduce radical flux rates in CS from the kinetic curves.

Conclusions – Preliminary results show that there are 2.6 nmol/puff radicals in whole smoke generated from a commercial brand cigarette. Further work is under way to improve the system for optimal radical trapping capacity and eliminate possible interferences from other components in the smoke.

The Formation of Radicals by Oxygen Chemisorption in Charred Burley Tobacco

Ji-Wen Feng* and **Jan B. Wooten**
Philip Morris USA, Richmond, Virginia

Using EPR spectroscopy, Feng and Maciel (1) have recently shown that polysaccharides such as pectin and cellulose when heated under inert atmosphere at temperatures between 300 – 400 °C form chars that exhibit an increase in radical concentration when the freshly prepared samples are exposed to air at room temperature. The EPR g-values of these so-called "new" radicals show that they differ in composition from the stable radicals associated with the large clusters of polycyclic aromatic rings found in chars of organic materials. The g-values indicate that the radicals are oxygen-rich or oxygen-centered radicals. It was also observed that the creation of these new radical species is mediated by the presence of alkali and alkaline earth metal ions such as Na, K, and Ca; chars of pure cellulose, for example, do not exhibit the effect. The most abundant metal ions in plants are K, Ca, and Mg. These results suggest that chars of heated plant material should also exhibit of oxygen chemisorption to form new char radicals. To test this hypothesis, cured Burley tobacco was heated in a tube furnace under He at 350 for 1 hr. The sample under helium was placed in the EPR spectrometer and monitored as function of air exposure time with the EPR tube cap removed. For up to 16 hours, the EPR signal increased with air exposure time and then very slowly declined. The total increase in the number of spins was ca. 5.6×10^{18} over the baseline aromatic radical concentration of 3.9×10^{18}. To test whether the change in radicals was influenced by metal ions, the sample was washed with water and acid. The water extraction removes most of the K and Mg ions leaving only ca. 0.8 wt % of Ca (compared to 3.2 % in the starting material). The sample was heated under identical conditions and examined by EPR. The extracted sample showed an increase in radicals, albeit reduced to an increase of only 1.8×10^{18} spins.

The results of the tobacco EPR study show that the endogenous metal ions promote the formation of oxygen-centered radicals in heated tobacco in the presence of air. The laboratory experiments suggest that these radicals form in the char of smoking cigarettes. The oxygen-centered radicals may lead to the evolution of oxygen species such as CO, phenols and other dihydroxy benzenes, semiquinone radicals or other species in cigarette smoke.

Reference

Ji-Wen Feng and Gary E. Maciel, "EPR Investigations of the Effects of Inorganic Additives on the Charring and Char Oxidation of Cellulose," submitted to *Fuel & Energy*, **2003**.

* Visiting Scientist from the Wuhan Institute of Physics, Wuhan, China

In-Situ High-temperature EPR Investigations of the Charring and Char Oxidation of Cellulose, Cellulose/Na_2CO_3 Mixtures and Tobacco

Shaokuan Zheng, Ji-Wen Feng, and **Gary E. Maciel**
Department of Chemistry, Colorado State University, Ft. Collins, Colorado

In–situ high-temperature EPR has been used to study the pyrolysis of cellulose and tobacco and oxidation of the resulting chars, as well as the influence of the inorganic additive, Na_2CO_3, on cellulose pyrolysis. It has been found that the addition of Na_2CO_3 not only dramatically changes pyrolysis behavior, but also has substantial effects on the subsequent oxidation of the resulting chars. The presence of Na_2CO_3 substantially narrows the EPR linewidth of cellulose chars for charring temperatures $\geq$ 375 °C. For the cellulose/Na_2CO_3 sample, pyrolysis at 375 °C leads to a very narrow EPR line of 1.0 G, while such a narrow EPR line can be observed only at pyrolysis temperature > 500 °C for pure cellulose. The high-temperature oxidation of cellulose/Na_2CO_3 chars or tobacco chars involves two different types of chemical transformations, the *production* and *annihilation* of free radicals. Only a small amount of surface free radicals are produced by the isothermal oxidation of pure-cellulose chars, relative to the case of cellulose/Na_2CO_3 chars. The possible interference of tar signals in these EPR studies has been examined and apparatus modifications are addressing this issue.

^{13}CO and $^{13}CO_2$ Carbon-13 Magnetic Resonance Imaging (MRI) Gas-Phase Measurements as a Function of Temperature and Concentration Measured in the Presence/Absence of a Nanophase Transition Metal Oxide Catalyst

David E Axelson[1] and Firooz Rasouli[2]
[1]MRI Consulting, Kingston, Ontario, Canada
[2]Philip Morris USA, Richmond, Virginia

Hypothesis: Nanophase transition metal oxides, with small particle size and high surface area, could potentially provide significantly improved catalytic performance over non - bulk catalysts candidates for removal of carbon monoxide in a burning cigarette. One such nanoparticle metal oxide is NANOCAT® Superfine Fe_2O_3 nanoparticles. Its catalytic activity for carbon monoxide oxidation has only been recently evaluated [1]. In this preliminary work, NANOCAT® CO catalysis was evaluated from direct ^{13}C MRI observation of the ^{13}C-enriched gases (^{13}CO, $^{13}CO_2$). The ultimate goal is to achieve, as much as possible, real time dynamic characterization of the gas kinetics/concentrations during catalysis in a cigarette.

Results: Initial studies required assembling extensive information regarding the temperature and concentration dependence of the magnetic resonance behavior of the gases, as these systems have never been studied before. It was determined that chemical shift differences under the experimental conditions used are sufficient to allow clear discrimination between CO and CO_2 signals in mixtures at any temperature relevant to this study. Furthermore, relaxation time variations between the gases are sufficiently large that either gas may be selectively monitored without interference from the other. The spin-echo, single point imaging (SESPI) protocol was found to work best to date. Limits of detection for CO and CO_2 were determined.

Conclusions: Preliminary dynamic ^{13}C MRI measurements of CO catalysis have been demonstrated. The factors that must be addressed to reduce the measurement times have been identified.

[1] Ping Li, Donald E. Miser, Shahryar Rabiei, Ramkuber T. Yadav, Mohammad R. Hajaligol, Applied Catalysis B: Environmental 43 (2003) 151–162

Detailed Mechanism of Formation of Gas-Phase and Volatile Products from the Pyrolysis of Glycerin and D-Glucose as Elucidated by the use of Isotopic Labeling with Carbon-13

John B. Paine III, Yezdi Pithawalla, John D. Naworal, and Charles E. Thomas, Jr.
Philip Morris USA, Richmond, Virginia.

Flash pyrolysis of specifically labeled glycerin and D-glucose, followed by GC/MS analysis, was used to identify the products, determine the overall extent of isotopic incorporation, and location of label within the molecule. Such information allows the determination of location of origin of pyrolysis products from within the parent molecules. Knowledge of the specific origin of products allows strong deductions to be made as to the mechanistic processes involved in their formation. Pyrolysis of a blend of natural-abundance and uniformly labeled substrate showed that typically more than 80% of any given product (except benzene) not containing more carbons than the precursor arose in unimolecular fashion, as evidenced by a relative lack of isotopic scrambling.

Pyrolysis of glycerin showed that acetaldehyde arose unimolecularly by two competing mechanisms. C-2 of glycerin became the aldehyde group as a result of Mechanism A, or the methyl group as a result of Mechanism B. Mechanism A is rationalized as involving hydrogen-bonding between the hydroxyl-groups at C-1 and C-3, and a concerted electrocyclic fragmentation into enol-acetaldehyde, formaldehyde and water. Mechanism B, found to be favored by the presence of potassium salts, likely involves hydrogen-bonding between the hydroxyl-groups at C-1 and C-2. Alkali cation-assisted hydride migration from a terminal hydroxymethyl group (or its alkoxide anion equivalent) displaces the central hydroxyl-group by nucleophilic displacement, in an alkaline version of the pinacol rearrangement. The resulting 3-oxo-1-propoxide anion undergoes a thermal retro-Aldol cleavage to afford formaldehyde and acetaldehyde enolate.

The large number of 1,2- and 1,3-diol interactions possible with carbohydrates means that these two mechanisms can provide numerous sites of initial bond-breakage when such molecules are pyrolyzed. These initial cleavage reactions, followed by likely further transformations of the initial products, will be shown to rationalize a significant number of important labeling patterns found among the volatile products of glucose pyrolysis. The origins of formaldehyde, acetaldehyde, acrolein, formic acid, acetic acid, glycolaldehyde, pyruvaldehyde (methylglyoxal), furfural, 1-hydroxy-3-buten-2-one, methacrolein, crotonaldehyde and methyl vinyl ketone will be discussed.

Formaldehyde Formation from Mainstream Smoke Gas Phase Aging

San Li, Joseph L. Banyasz and Ken H. Shafer
Philip Morris USA, Richmond, Virginia.

When the gas phase of cigarette mainstream smoke was isolated in a closed container and aged, formaldehyde formation was observed. The increase of formaldehyde in the mainstream smoke gas phase as a function of aging time was accompanied by decrease of isoprene and NO, monitored simultaneously in real time by Fourier transforms infrared spectroscopy (FTIR) technique. To understand this experimental observation, a gaseous mixture of isoprene, nitric oxide and air was trapped inside an infrared gas cell and very similar spectroscopic behaviors were found as that in aged gas phase smoke. Experiments with different isoprene/NO/air mixing ratios as well as at different temperatures were performed and the results on the reaction products and possible reaction mechanism will be discussed.

A Multivariate Interpolation Scheme for the Functional-Group Biomass Pyrolysis Model (FG-BioMass)

Eric P. Rubenstein, **Marek A. Wójtowicz**, Elizabeth Florczak and Michael A. Serio
Advanced Fuel Research, Inc., East Hartford, Connecticut

Hypothesis: An interpolation scheme for the FG-BioMass pyrolysis model makes it possible to create input files for the model on the basis of easily measurable properties, such as elemental composition and proximate analysis. Input files created by the interpolation program can be used to predict pyrolysis-product evolutions as a function of thermal history of the biomass sample.

Results:

- A multivariate linear least-squares technique was developed to interpolate input parameters for a tobacco sample using a database of 11 tobacco samples.
- The database was created using TG-FTIR experiments at three heating rates for each biomass sample (10, 30, and 100 K/min).
- For each biomass sample, a kinetic analysis was performed based on first-order parallel reactions with Gaussian distributions of activation energies. Sizes of precursor pools were determined for each species. Tar evolution was treated as a process that is independent of the evolution of other volatile species. This information was used to prepare FG-BioMass input files for each sample included in the database.
- The following biomass characteristics were considered as possible inputs for the interpolation program: C, H, O, N, S, K, Ca, Na, Mg, ash, and volatile matter (VM).
- In a number of runs, different samples from the database were treated as biomass with unknown pyrolysis behavior, but known elemental composition and proximate analysis.
- For each evolution peak (precursor pool), the following parameters were determined by the interpolation program: (1) the pool size; (2) mean activation energy; (3) pre-exponential factor; and (4) width of the Gaussian distribution of activation energies. This information was used to prepare an FG-BioMass input file, which was then compared to the input file created on the basis of TG-FTIR experiments. Errors associated with the use of the interpolation scheme were computed for each set of input parameters (e.g., [C, H, O, VM]).

Conclusions:

- It was found that adding parameters to the baseline case of [C, H, O] reduced interpolation error (e.g., by up to a factor of 8 for Oriental tobacco).
- In most cases studied, the best set of input parameters was found to be [C, H, O, Ca, ash, VM].

Quad Quantum Cascade Laser Spectrometer for Simultaneous Analysis of Mainstream and Sidestream Cigarette Smoke

Randall Baren[1], Milton Parrish[1], Ken Shafer[1], Charles Harward[2], Q. Shi[3], D. Nelson[3], B. McManus[3], and M. Zahniser[3]
[1]Philip Morris USA, Richmond, Virginia.
[2]Nottoway Scientific Consulting Corp., Nottoway, Virginia
[3]Aerodyne Research, Inc., Billerca, Massachusetts

Hypothesis: To develop an analytical technique using high resolution infrared spectroscopy that can monitor the formation of selected gaseous constituents simultaneously in mainstream and sidestream cigarette smoke.

Results: A compact, fast response, infrared spectrometer using four pulsed quantum cascade (QC) lasers has been applied to the analysis of gases in mainstream and sidestream cigarette smoke. QC lasers have many advantages over the traditional lead salt lasers, including near-room temperature operation with thermoelectric cooling and single mode operation with improved long-term stability. The new instrument uses two 36 m, 0.3 liter multiple pass absorption gas cells to obtain a time response of 0.1 seconds for the mainstream system and 0.4 seconds for the sidestream system. With this instrument we have measured simultaneously in mainstream and sidestream smoke the concentrations of ammonia, ethylene, nitric oxide, and carbon dioxide. Also, simultaneous measurements of CO_2 from a non-dispersive infrared analyzer are used to obtain emission ratios of the smoke constituents relative to the amount of CO_2 produced during combustion for various types of cigarettes.

Conclusions: A data rate of 20 Hz provides sufficient resolution to reveal the concentration profiles during each 2-s puff in the mainstream smoke. Different concentration profiles before, during and after the puffs have also been observed for these smoke constituents in the sidestream smoke.

Development of GC-Combustion-Isotope Ratio Mass Spectrometry for Analysis of PAHs in Mainstream Smoke: Investigation of Precursor-Product Relationships

Phillip F. Britt, A. C. Buchanan III, Roger A. Jenkins, Deon Bennett, and J. Todd Skeen
Chemical Sciences Division, Oak Ridge National Laboratory, Oak Ridge, Tennessee

Hypothesis: Gas chromatography-combustion-isotope ratio mass spectrometry (GC-C-IRMS) will be used to determine the precursors to polycyclic aromatic hydrocarbons (PAHs) in mainstream cigarette smoke by spiking cigarettes with ^{13}C-labeled tobacco components and analyzing the ^{13}C content of the PAHs in the total particulate matter by GC-C-IRMS.

Results: Initially, a clean up procedure had to be developed for separation of the PAHs from the total particulate matter (TPM) of 2R4F cigarettes. Although PAHs in TPM are routinely quantitated by GC-selective ion monitoring mass spectrometry and HPLC with fluorescence detection, these methods conveniently ignore coeluting impurities. To obtain the highest sensitivity in the isotope ratio measurement, no other components can coelute with the PAHs of interest, making the sample clean up more challenging. Mainstream cigarette smoke was generated with a 20-port smoking Philip Morris machine using Federal Trade Commission conditions: 2-second duration, 35-mL puff once per minute on ISO-conditioned cigarettes. The PAHs were isolated from the TPM of 120 cigarettes by water washing, followed by solid phase extraction using a silica cartridge and an aminopropyl modified silica cartridge, followed by semi-prep HPLC on an aminopropyl modified silica column, and GC analysis. Although the final samples are still very complex, phenanthrene, benz[a]anthracene, chrysene, benzo[a]pyrene, benzo[e]pyrene, and the benzofluoranthene isomers are cleanly separated from the other components on the GC column. Standards were also added to the TPM so the recovery of PAHs could be followed.

A GC-combustion apparatus was connected to an existing IRMS at ORNL for the analysis of the PAHs. To optimize the GC separations and troubleshoot resolution issues, a flame ionization detector was added to the GC. We have been able to reproducibly measure isotope ratios (±2%) on pure samples of phenanthrene, benz[a]anthracene, and benzo[a]pyrene at levels as low as 0.3 nmol (6-8 ng) and we have obtained linear response over two orders of magnitude. In practice, GC-C-IRMS can routinely detect $^{13}C/^{12}C$ of ca. 0.00001 on approximately 5-10 ng of sample. We are currently optimizing GC-C-IRMS parameters for the analysis of PAHs isolated from TPM. Once successful, the TPM of cigarettes spiked with ^{13}C-labeled tobacco components, such as cholesteryl stearate (3,4-$^{13}C_2$) and glucose-$^{13}C_6$, and unlabeled components will be investigated by GC-C-IRMS.

Conclusions: This study will address an unresolved 50-year old question as to the importance of tobacco hydrocarbons in the formation of PAHs. This study will

provide precursor-product relationships for PAHs and potentially nitrogen containing polycyclic aromatic compounds (N-PACs), since $^{15}N/^{14}N$ measurements can also be made with this instrument. From the combustion and pyrolysis of ^{13}C-labeled tobacco components and tobacco, experimental conditions can be found to simulate the product yields and distributions found in a burning cigarette, so that model compound studies can be related to smoking studies. This research will also provide new insights into the reduction of PAHs and *N*-PACs in mainstream cigarette smoke.

Maillard Chemistry in Char Maturation: Comparison of Different Amino Acids

Mark Nimlos, Thomas Sherow, Karl Andreason, Mike Looker,
Bob Evans, and Luc Moens
National Renewable Energy Laboratory, Golden, Colorado

Hypothesis: The amino acids found in tobacco interact with carbohydrates by mechanisms known as Maillard chemistry. The maturation of char during pyrolysis and the gaseous emissions are dependant upon the structure and reactivity of the amino acid. We have investigated the pyrolysis of four amino acids mixed with carbohydrates in an attempt to understand how differences in Maillard chemistry can effect the maturation of char and the emissions of PAHs and other volatile compounds of interest. Four amino acids (proline, asparagines, aspartic acid and tryptophan) were mixed with simple carbohydrates (glucose and glyceraldehydes) and a carbohydrate matrix (glucose, pectin and cellulose) and were pyrolyzed at different temperatures. A slide-wire reactor was used to investigate the effects of sequential temperature ramps upon product formation. Gaseous products are measured with our Molecular Beam Mass Spectrometer (MBMS) and char is analyzed with FTIR.

Results:

1. Proline appears to be the most reactive of the amino acid of those tested. This high reactivity is likely due to its unique molecular structure and is consistent with literature reports using proline as aldol reaction catalyst.
2. Maillard chemistry appears to affect the rate of maturation of the char with the higher reactivity leading to the formation aromatic functionalities at lower temperatures.
3. Proline reactions lead to the formation of a complex suite of high molecular weight gas phase products, which may contain aromatic compounds.
4. The existing aromatic rings in tryptophan appear to be the nucleus for the formation of larger aromatic species in the gas phase.
5. For tryptophan and proline the thermal history of the char can affect the evolution of gas phase products.

Conclusions: The types of amino acids present in biomass should affect the rate of formation and the stability of the char, which could lead to changes in the formation of PAHs during the pyrolysis/combustion of the char. A highly reactive amino acid, such as proline, will have a significant impact upon char stability when subsequently exposed to higher reaction severity.

Phenolic Compound Formation from Tobacco and Tobacco Components

Thomas E. McGrath, Raquel M. Olegario, Gayle M. Powers and W. Geoffrey Chan
Philip Morris USA, Richmond, Virginia.

Hypothesis: Can oxidative pyrolysis experiments of tobacco be used to study the formation of phenolic compounds from a burning cigarette? If so, what are the predominant components of tobacco that give rise to phenolic compounds such as hydroquinone and catechol?

Key Results:

- Oxidative Pyrolysis can be used as a model to study the formation of phenolic compounds. This allows one to study the effect of sample size, gas phase residence time, O_2 concentration, heating rate, NH_3 concentration, temperature evolution profiles, and solvent extraction, on the formation of phenolic compounds from tobacco and tobacco components.
- Hydroquinone and catechol are formed predominantly below 350 °C
  - chlorogenic acid and rutin appear to be the main precursors
- Methyl catechols, resorcinol and cresols are formed predominantly above 350 °C
  - tobacco char appears to be the main precursor
- Not a significant effect of: sample size
  gas phase residence time
- Significant effect of O_2 on Phenolic yields:

Decrease in:	Increase in:	Unchanged:
hydroquinone	3 methylcatechol	Phenol
catechol	4 ethylresorcinol	Cresols

- Cold water extraction significantly reduces the yield of hydroquinone (80%), phenol (52%) and catechol (32%) but increases the yields of resorcinols and methylhydroquinone

Conclusions: Oxidative pyrolysis of tobacco has been shown to be a good experimental model for the study of phenolic compounds from a burning cigarette. The detection and quantification of phenolic compounds present in tars derived from tobacco and tobacco related components may potentially be correlated to the cytotoxicity of the same tars.

Conclusions Regarding the Product: An understanding of phenolic formation precursor relationships may lead to the development of a reduced phenolic yielding lit end cigarette. Hydroquinone is predominantly formed from water soluble precursor(s) and selective removal/reduction of the precursor(s) should result in lower yields from a burning cigarette.

Reduction of Catechol and Hydroquinone by Catalyst and Ammonia

Eun-Jae Shin, W. Geoffrey Chan, Firooz Rasouli and Mohammad R. Hajaligol
Philip Morris USA, Richmond, Virginia.

Hypothesis I: Iron oxide nano-particles, as a catalyst, may catalytically convert or oxidize phenolic compounds such as catechol and hydroquinone to other benign products.

Results I:

- Significant conversion of catechol and hydroquinone was observed at temperatures as low as 230°C and 180°C, respectively.
- Three classes of products, primary, secondary and tertiary were extracted from both cracking reactions by using factor analysis.
- As temperature increases, tertiary products, which were carbon dioxide and water became dominating products for both cracking reactions.
- For catechol, the activation energy over iron oxide was reduced by factor of 2, compared to pure pyrolysis reaction.

Hypothesis II: Ammonia may suppress the formation of phenolic compounds such as catechol and hydroquinone during the pyrolysis of their possible precursor, e.g. chlorogenic acid.

Results II:

- Heating pure catechol and hydroquinone in the presence of ammonia may form an unknown product, a peak at m/z 127.
- The formation of catechol and/or hydroquinone in the presence of ammonia was suppressed during the pyrolysis of chlorogenic acid.
- For chlorogenic acid, pyrolysis products with odd masses were observed in the presence of ammonia indicating the possible formation of nitrogen containing compounds.

Conclusions: Iron oxide nano-particles may act as a catalyst and ammonia as an inhibitor to reduce phenolic compounds such as catechol and hydroquinone during the thermo-chemical processes.

Characterization of the Particle Size Distribution of Mainstream Cigarette Smoke

David Kane and Peter Lipowicz
Philip Morris USA, Richmond, Virginia.

Hypothesis: Due to the high particle number density of mainstream cigarette smoke conventional methods for measuring aerosol particle size distributions cannot be applied without significant dilution of the smoke prior to measurement. Dilution and the time required to make the measurement may result in changes in the particle size distribution. Undiluted smoke may be sized in real-time by ensemble light scattering or light extinction methods. However, these methods require a complicated inversion of the scattering or extinction data to determine the aerosol size distribution and may produce unreliable results. As both approaches have their own strengths and limitations they may be applied as complimentary techniques.

Results: Two methods for characterizing the particle size distribution of mainstream cigarette smoke are under development. The first uses a well characterized, commercially available instrument called a scanning mobility particle sizer (SMPS). The second uses a light extinction method previously developed by Ken Cox and Tung Nguyen.

The SMPS system requires approximately 500x dilution of the cigarette smoke prior to the measurement. At this dilution level agglomeration of the particles can still increase the particle size over the ~2 minutes required to complete the measurement. Furthermore, dilution may result in the evaporation of the more volatile species, such as nicotine, from the particle decreasing the average particle diameter.

The light extinction method can directly size the smoke without dilution and with a time resolution greater than 0.1s, fast enough to make intrapuff measurements possible. However, the inversion of the extinction data to determine the particle size distribution does not provide a unique solution and assumptions about the shape of the distribution must be made. A simple method has been applied to estimate the particle size distribution from the light scattering data.

Conclusions: The application of two independent methods to measure the particle size distribution of cigarette smoke provides complimentary data. In particular the SMPS measurement, which has previously been determined to be extremely reliable, can be used to validate the light extinction method. Due to its ability to rapidly make measurements the light extinction method can provide unique intrapuff data.

The Identification of Nitro Polycyclic Aromatic Hydrocarbons in Tobacco Smoke Using Electron Monochromator Mass Spectrometry

John Dane[1], Kent J. Voorhees[1], Crystal Havey[1], Christy Abbas-Hawkes[1], and Robert B. Cody[2]

[1]Department of Chemistry and Geochemistry, Colorado School of Mines, Golden, Colorado

[2]JEOL USA, Peabody, Massachusetts

Hypothesis: The use of GC-EM/MS is an effective technique for the identification of nitro-substituted polycyclic aromatic hydrocarbons (NPAHs) in mainstream tobacco smoke.

Results: A methodology will be presented that is specific and highly sensitive for NPAHs in mainstream tobacco smoke. This approach utilizes a combination of multiple separation steps to isolate the NPAHs from the smoke in conjunction with a GC-MS system equipped with an electron monochromator (EM) ionization source. In principle, because of the ability of the EM to preferentially ionize the NPAHs, greater specificity should be attained during the analysis of complex mixtures. Empirical data using standard NPAHs indicate that the nitro constituents of most nitro-aromatic compounds have an electron capture resonance in the 3-4eV range. Therefore, using the GC-EM/MS system to analyze the mainstream tobacco smoke, NPAHs are tentatively identified by the emergence of a nitro (NO_2^-) mass spectral peak at m/z 46 when an electron ionization beam of 3.5eV is used. Additionally, these compounds produce molecular radical anions at near 0eV electron energies. The correspondence in retention times between the m/z 46 anion peaks at electron energy of 3.5eV and the molecular anion peaks at near 0eV provides information suitable for identifying the NPAHs found within a smoke sample. The result of monitoring the m/z 46 anion using the GC-EM/MS clearly shows the presence of a number of NPAHs in mainstream tobacco smoke. Of these, several NPAHs have been further identified through their molecular ion information. The NPAHs identified thus far have up to four rings present within the structure, making this the first work to show the presence of multi-ring nitro-aromatics in mainstream tobacco smoke.

Conclusions: While further optimization of the separation steps is necessary to increase the recovery of all NPAHs present within the mainstream tobacco smoke, the data collected to this point indicate the use of GC-EM/MS is an effective technique for the elucidation of NPAHs in mainstream tobacco smoke.

Vapor Pressures of Tobacco Tar Related Materials

Vahur Oja[1] and Mohammad R. Hajaligol[2]
[1]Department of Chemical Engineering, Tallinn Technical University, Tallinn, Estonia
[2]Philip Morris USA, Richmond, Virginia.

Hypothesis: The information on tobacco tar vapor pressures is useful knowledge for smoke aerosol related engineering calculations. For example, the knowledge can be applied in modeling cigarettes under burning and smoldering conditions or in predicting the behavior of environmental smoke contaminants. Past studies have shown the need of the reliable of vapor pressure information on tobacco tar and heterogenic complex tobacco tar related materials at low and at high temperatures.

Results:

1. Vapor pressures experiments on several classes of pure compounds were performed to improve our understanding concerning the intermolecular forces present in tobacco tars. The aim was to obtain reliable data with the scientific value. These data show very complex vapor pressure behaviors of selected heteroatom rich compounds. The experiments also show that due to thermal behavior of compounds the experimental techniques can not provide desired vapor pressure data on all desired materials or/and over the temperature region of interest.

2. Vapor pressure estimation methods (group contribution, empirical correlations, quantum chemistry based) were utilized to estimate vapor pressures of complex tobacco related compounds near or beyond the melting point, from melting point to boiling point and even higher. Although, these methods often have limited accuracy or the accuracy of such prediction is unknown, they still can provide useful information on vapor pressure magnitudes for pyrolysis modeling.

Conclusion: Combination of experimental data and results from estimation techniques can provide useful vapor pressure information on tobacco tars and structurally complex hydrocarbons related to tobacco tars at operating conditions of interest.

Pyrolysis and Oxidation of Biomass with Nanoparticle Iron Oxide: The Catalytic Effects on CO, NO, Tar and the Reaction Mechanisms

Ping Li, Firooz Rasouli, and Mohammad R. Hajaligol
Philip Morris USA, Richmond, Virginia.

Hypothesis: Nanoparticle iron oxide is an effective catalyst for CO, NO, and Tar, etc. in pyrolysis/oxidation process of biomass.

Results:

1. CO/NO removal.
   - In the sequential pyrolysis and char oxidation process, mixing 10% of nanoparticle iron oxide with biomass removed 59% of CO and 33% NO. The reductions largely occurred in char oxidation step. In the simultaneous pyrolysis and oxidation process, 60% of CO and 51% of NO were removed.
2. Extra CO_2 production and tar loss.
   - Biomass mixed with nanoparticle iron oxide produced more CO2 than what can be accounted for by the reduction in CO. The extra CO2 production was correlated to the 21% loss of tar. However, in the oxidation of biomass char mixed with the FRESH nanoparticle iron oxide, CO, NO were reduced, but no extra CO2 production was observed. It confirmed the loss of tar was the source of extra CO2.
3. Catalytic oxidation of CO.
   - Nanoparticle iron oxide was an effective CO catalyst and the coating of the biomass tar did not deactivate the catalyst.
4. NO removal mechanisms.
   - The reduced form of nanoparticle iron oxide catalyze the CO + NO = N2 + CO2 reaction under the O2 deficient conditions.
   - Pre-mixed nanoparticle iron oxide with biomass promote 2NO + C (char) = N2 + CO2 reaction.
   - Iron reacted with the nitrogen containing char to form iron nitrides, which further decomposed to N2 and iron (from reference)
5. Effect on tar composition.
   - The effects of nanoparticle iron on the changes of tar composition were evaluated and analyzed.

Conclusions: Mixing nanoparticle iron oxide with biomass was effective in removing CO/NO in the oxidation/combustion processes. Tar loss was correlated to the extra CO_2 production and changes of tar composition were analyzed. The CO removal was through catalytic CO oxidation. The NO removal involved several possible mechanisms.

Investigation of Adsorbents for the Selective Filtration of Gas-phase Components in the Cigarette Smoke

Mark S. Zhuang, Diane Gee, Jose Nepomuceno, and George Karles
Philip Morris USA, Richmond, Virginia.

Hypothesis: The pore size distribution, pore volume and molecular make-up of an adsorbent affect the adsorption capacity and adsorption selectivity of gas-phase components in the cigarette smoke. Most of activated carbons have high surface area and majority of the pores are micropores (with pore width less than 20 Å). The surface of activated carbons is commonly non-polar and therefore activated carbons should be more effective to adsorb weak polar gas-phase molecules. Silica gels on the other hand, have large pore volumes but relatively lower surface area compared to activated carbons. This is because majority of the pores in silica gels are meso-pores (with pore size between 20 to 500 Å). The surface of silica gels is more polar compared to that of activated carbons and thus silica gels should be more effective to remove strong polar molecules. The gas-phase components in the cigarette smoke are low boiling-point species and are believed to be light molecules; we postulate that adsorbents with large volume of micro-pores are more effective to remove these molecules.

Results: Three commercially available adsorbents, petroleum pitch based activated carbon beads, coconut shell based activated carbon granules and spherical silica gels were used in this study. The surface properties of these three adsorbents were measured using a Micromiretics Porosimeter. Results showed that the BET specific surface areas for the pitch-based carbon, coconut shell-based carbon and silica gel were 1200, 1550 and 400 m^2/g, respectively, and total pore volumes were 0.51 cc/g, 0.59 cc/g and 0.95 cc/g, respectively. Majority of the pores in two activated carbon samples were micro-pores, while the silica gel contained meso-pores only. Mercury porosimetry data showed that the coconut shell-based carbon had large volume of macro-pore as compared to the pitch-based carbon. This confirmed by the bulk density data of these two carbon samples – the coconut-shell based carbon had a bulk density of 0.38 g/cc vs. 0.59 g/cc for the pitch-based carbons beads. Each adsorbent was incorporated into cigarette filters with a plug-space-plug configuration; combinations of two adsorbents were also incorporated into cigarette filters with a plug-space-plug-space-plug configuration. A puff-by-puff GC/MS was used to measure the smoke chemistry for the filtration efficiency. Results showed that the overall delivery of the gas-phase components were much smaller for the filters containing the activated carbons compared to those containing silica gels. For silica gels, the reduction of formaldehyde, hydrogen cyanide, and hydrogen sulfides was relatively higher as compared to the reduction of other less polar components in the same smoke stream. The combination of silica gel and activated carbon in a cigarette filter did not provide significant impact on the selectivity. The filtration efficiency of activated carbon was much higher than that of silica gel and the activated carbon became the dominating factor affecting the removal of the gas-phase components.

Conclusions: Microporous materials are more effective to remove the gas-phase components in the cigarette smoke than mesoporous materials. Silica gels are more selective to remove polar gas-phase components in the cigarette smoke.

Sequential Oxidation of Metal Clusters

Purusottam Jena
Department of Physics, Virginia Commonwealth University
Richmond, Virginia

Using photoelectron spectroscopy and calculations based on density functional theory, we have systematically investigated the electronic structure of W and Au clusters interacting with atomic and molecular oxygen. The studies are aimed not only at understanding the effect of sequential oxidation on the properties of metal clusters but also on shedding light on the evolution of bulk properties as metal-oxide clusters grow. We show that the onset of oxide-like behavior of light on the evolution of bulk properties as metal-oxide clusters grow. We show that the onset of oxide-like behavior of W_4O_m-($0<m=6$) clusters occurs at m=5, well below the bulk stoichiometric composition (W_4O_{12}). The signature of this onset is established from a systematic study of the vertical detachment energies (VDE), adiabatic electron affinities (AEA), and the energy gaps between highest occupied (HOMO) and lowest unoccupied molecular orbitals (LUMO). An anomalous increase in the VDE, AEA, and HOMO-LUMO gap at m=5, accompanied by the cleavage of 50% of the W-W bonds and localization of electron charge density bear testimony for a transition from metal-like to oxide-like behavior. Similar studies also show that, contrary to the conventional understanding that atomic clusters usually differ in properties and structure from the bulk constituents of which they are comprised, a small cluster containing only 4 tungsten and 12 oxygen atoms bears all the hallmarks of crystalline tungsten oxide, WO_3. This observation based on a synergistic approach involving mass distributions under quasi-steady state conditions, photo-electron spectroscopy, and first principles calculations illustrates the existence of a class of materials whose embryonic forms are tiny clusters. We will also discuss the oxidation of gold clusters with atomic and molecular oxygen where an oxygen molecule is found to bind to a single Au anion dissociatively while it binds molecularly to larger Au anionic clusters as well as to all neutral Au clusters including a single Au atom. The relevance of these studies to a fundamental understanding of catalysis will be discussed.

Catalysis Study from First principles: CO oxidation on Au/TiO_2 (110), CO and NO reaction on Pd clusters

Xueyuan Wu[1], Annabella Selloni[2], Michele Lazzeri3,Joshua Whitney[1], Yiming Zhang[1] and **Saroj K. Nayak**[1]

[1] Department of Physics, Applied Physics and Astronomy
Rensselaer Polytechnic Institute, Troy, New York

[2] Department of Chemistry, Princeton University, Princeton, New Jersey

[3]Laboratoire de Mineralogie Cristallographie de Paris, Paris, France

One of the key processes in CO oxidation is the oxygen adsorption and desorption at finite temperature. Using first principles density functional calculations and Car-Parrinello scheme we have studied the interactions of molecular oxygen with a partially reduced rutile TiO_2 (110) surface. In agreement with experiments, a number of different O_2 adsorption states, both molecular and dissociated, have been found. The kinetic barriers for conversion between these states have been also calculated. Based on these results, we analyze the mechanism of oxygen vacancy diffusion, recently observed by Scanning Tunneling Microscopy (STM), and suggest a new pathway which does not imply the high oxygen adatom reactivity assumed in the original model.

The reactivity of the stoichiometric and partially reduced rutile TiO_2 (110) surfaces towards oxygen adsorption and carbon monoxide oxidation has been studied by means of periodic density functional theory (DFT) calculations within the Car-Parrinello approach. O_2 adsorption as well as CO oxidation are found to take place only in presence of surface oxygen vacancies (partially reduced surface). The oxidation of CO by molecularly adsorbed O_2 at the O-vacancy site is found to have an activation energy of about 0.4 eV. When the adsorbed O_2 is dissociated, the resulting adatoms can oxidize incoming gas-phase CO molecules with no barrier. In all studied cases, once CO is oxidized to form CO_2, the resulting surface is defect-free and no catalytic cycle can be established. We show adsorbing Au/TiO_2 surface allows a complete CO oxidation process. Finally we have studied interaction of both CO and NO with Pd clusters to understand the CO-NO reaction.

Metal Oxide Catalyst of CO/NO to CO_2/N_2: Fe_mO_n and Cu_mO_n Nanoparticles

Elliot R. Bernstein, D. N. Shin and Y. Matsuda
Department of Chemistry, Colorado State University, Fort Collins, Colorado

Little is known in detail concerning the heterogeneous catalytic process in terms of electronic and geometric structure of the active catalytic site and the actual step-by-step mechanism for the catalytic reaction. This fundamental problem is addressed within the context of the catalysis of the reaction $2CO + 2NO \rightarrow 2CO_2 + N_2$ by iron oxide and/or copper oxide. Our approach to solving this fundamental problem is to generate neutral nanoparticles of metal oxides in the gas phase, pass them through a reaction cell filled with various concentrations of CO and/or NO, and search for products and changed clusters. The underlying assumption of this study is that, as the nanoparticles sweep through different sizes and geometries (e.g., Fe_mO_n, Cu_mO_n), all potential condensed phase reactive sites will be generated: mass and optical spectroscopy, along with calculation, will be able to reveal the active species for the heterogeneous catalytic conversion of CO/NO to CO_2/N_2. We have determined the neutral cluster distribution for both sets of metal oxide nanoparticles and we are now studying their reactivity. The first systems we have explored are Fe_mO_n + NO and Fe_mO_n + CO. We have observed N atoms and found that Fe_5O_5 seems to be particularly active because, as the NO and CO pressures increase in the reaction cell, the Fe_5O_5/Fe_mO_m ($m \leq 4$) intensity ratio increases. These data have been obtained with nanoparticle detection at 193 nm ionization energy. We are presently exploring reactions for both Cu_mO_n and Fe_mO_n clusters with various NO, CO, and NO/CO concentrations using 118 nm ionization for product and nanoparticle detection. We will discuss the implications of these results for the catalysis of the above reaction by iron and copper oxides.

Gold Nanoparticle Catalysts for Low Temperature CO Oxidation

Khaled Saoud[1], **M. Samy El-Shall**[1] and Sarojini Deevi
[1]Department of Chemistry, Virginia Commonwealth University, Richmond, Virginia
[2]Philip Morris USA, Richmond, Virginia.

Low-temperature catalytic oxidation of CO is one of the most important problems in catalysis since even small exposures to CO (ppm) are undesirable.

Nanoparticle catalysts are characterized by large surface area, high dispersion and strong metal-support interaction. It is therefore, expected that nanoparticle catalysts would show high catalytic activity for the low temperature oxidation of CO.

Using our Laser Vaporization Controlled Condensation (LVCC) method, we have prepared a variety of nanoparticle catalysts for the CO oxidation. Nanoparticle catalyst supports have been investigated to explore the advantage of strong metal-support interaction in developing new efficient catalysts. We have studied the effects of the nanoparticle supports of silica (SiO_2), alumina (Al_2O_3), titinia (TiO_2), zirconia (ZrO_2) and ceria (CeO_2) on the activity of the Au nanoparticle catalysts. The effects of metal loading and heating treatments have been investigated. The Au/ CeO_2 system shows a great promise for the efficient low temperature oxidation of CO. This appears to be directly related to the unique redox properties and high oxygen storage capacity of CeO_2.

Synthesis of Nanoscale Au/Fe_2O_3 Catalysts for CO Oxidation by Deposition-Precipitation Technique

Mikhail Khoudiakov[1], Mool C. Gupta[1], and **Sarojini Deevi**[2]
[1]Applied Research Center, Old Dominion University, Newport News, Virginia
[2]Philip Morris USA, Richmond, Virginia.

Hypothesis: Gold/iron oxide catalysts prepared by deposition precipitation and co-precipitation methods should show similar activity for CO oxidation

Results: Nanoscale Au/Fe_2O_3 catalysts for CO oxidation were prepared by deposition-precipitation technique using thermal decomposition of urea. Freshly precipitated amorphous $Fe(OH)_3$ was used as a support. The resulting products were characterized by transmission electron microscopy and X-ray powder diffraction. The catalysts in the "as prepared" state demonstrated exceptionally high activity toward CO oxidation. Compared to conventional coprecipitation with the same amount of gold precursor, the deposition-precipitation method was shown to produce more active catalysts because it allows complete precipitation of gold from solution.

Conclusion: Deposition-precipitation method using urea produces more active catalysts because it allows complete precipitation of gold from solution, and hence can be used for preparation of catalysts with efficient utilization of the precious metal reagents.

Evaluation of a Manganese Ferrite Based Mixed Oxide System as CO Oxidation Catalyst

S. PalDey, S. Gedevanishvili, and F. Rasouli
Philip Morris USA, Richmond, Virginia.

Commercially available black pigment consisting of mixed manganese, copper and iron oxides was tested as a catalyst for CO oxidation. The crystalline structure as detected by XRD was nonstoichiometric spinel oxide with a chemical formula of $Cu_{1.5}Mn_{1.5}O_4$ supported on Fe_2O_3. Earlier works report $CuMn_2O_4$ type spinel supported on alumina, active carbon and sodium carbonate. Little is known about Fe_2O_3 supported $Cu_{1.5}Mn_{1.5}O_4$ spinel. The fresh catalyst with irregular particles of 50-300 nm size range and a BET surface area of 18.5 $m^2\ g^{-1}$ was able to completely convert CO at 500°C even at a significantly high total CO-O_2-He gas flow rate of 1000 ml min^{-1}. Fresh catalyst is also an effective oxidant for carbon monoxide in absence of oxygen. While the reaction rate was independent of oxygen concentration (maintained above stoichiometric requirement), it depended on CO concentration. The reaction order over fresh catalyst was measured to be 0.57 with respect to CO with an apparent activation enthalpy of 26.53 kJ mol^{-1}. The lower value of activation enthalpy in this research as compared to earlier works on $CuMn_2O_4$ might be due to Fe_2O_3 support. Application of a reduction followed by oxidation type of heat treatment on fresh catalyst induced a less crystalline spinel structure with fine dispersion of metal oxides leading to a great improvement in catalytic activity. Complete CO conversion was achieved at 253°C (which is about 275°C lower than those of fresh catalyst) over heat treated catalyst. This shows how by designing a suitable heat treatment it is possible to tailor the structure and composition of catalyst to achieve optimum activity. TPR results indicate that the reduction of mixed spinel oxides occurs at lower temperatures than pure CuO, Fe_2O_3 and Mn_3O_4 suggesting their synergistic effect. Thus mixed oxides of transition metals can be a viable alternative of precision metal and noble metal containing catalysts for applications in relatively high temperatures such as for removing toxic CO gas from a burning cigarette.

Evaluation of Low Temperature Au/TiO_2 Catalyst for Removal of CO from Cigarette Smoke

Yezdi B. Pithawalla and Sarojini Deevi
Philip Morris USA, Richmond, Virginia

Hypothesis: The goal of this research is to evaluate the hypothesis that lower the light-off temperature of a catalyst the more efficient it is for removal of CO from cigarette smoke. If the above is not true can fundamental flow tube experiments be devised which help understand the reasons for the lower activity of the catalyst in a cigarette.

Results: Au dispersed on metal oxides are well known low temperature catalysts for the oxidation of CO. We used the deposition precipitation method to prepare several Au/metal oxide catalysts, where the metal oxide is either titania, alumina, zirconia, ceria or zinc oxide. Au/TiO_2 was selected to test the above hypothesis as it was found to have the lowest light-off temperature when tested for CO oxidation in a fixed bed continuous flow tube reactor. The Au/TiO_2 catalyst was active at sub-ambient temperatures and had a light-off temperature of 0°C. HRTEM and EDX analysis indicated that the Au/TiO_2 catalyst consists of Au nanoparticles approximately 2-3 nm in diameter, which were finely dispersed on the titania support. However the catalyst was less effective in the removal of CO from mainstream cigarette smoke. The above experiment proved that the suggested hypothesis is not true. Flow tube experiments were carried out in order to evaluate the contribution of factors listed below towards reducing effectiveness of the Au/TiO_2 catalyst for CO oxidation in a cigarette. Results on flow tube experiments which help understand the effect of moisture, absence of oxygen, effect of exposure of the catalyst to higher temperatures, poisoning by tar and light gases and the effect of the amount of catalyst used will be presented.

Conclusions: A lower light-off temperature in a flow tube experiment is not indicative of a higher efficiency of the catalyst for CO oxidation in a cigarette. Flow tube experiments provide an efficient way to single out multiple effects that may simultaneously contribute towards reducing the activity of a catalyst when used in a cigarette.

Feasibility of NO reduction via CO Oxidation: A Model Study for Iron-Oxide Particles

B. V. Reddy[1], F. Rasouli[1], and S. N. Khanna[2]
[1]Philip Morris USA, Richmond, Virginia.
[2]Physics Department, Virginia Commonwealth University, Richmond, Virginia

Hypothesis: Interaction of CO with NO occurs only at high temperature. An atomistic understanding of their adsorption and reaction mechanisms over catalytic sites, offers an indispensable approach for potential catalyst design to achieve the simultaneous oxidation and reduction of CO and NO respectively. Theoretical electronic structure studies have been carried out to investigate the NO reduction by CO over an isolated Fe_2O_3 cluster.

Results: Our studies, based on a first principles gradient corrected density functional approach, show that the direct reduction of NO by a Fe_2O_3 cluster is not feasible. However, the reduction is possible via an indirect pathway that involves the reduction of the Fe_2O_3 cluster. Here, an initial CO or NO adsorbed at the Fe site breaks one of the FeO bonds generating a low coordinated O atom. A second CO can be oxidized by the weakened O atom leaving the cluster and resulting in the reduced cluster. It is shown that this reduced CO-Fe_2O_2 can reduce NO. The reaction pathway is shown to proceed via an initial adsorption of the oncoming NO, weakening of the NO bond due to heat of adsorption and the oxidation of the CO by the weakened bond. The conditions favoring the reaction, the detailed reaction path, and the energetics of the reaction pathway will be highlighted. The theoretical findings will be compared with the available experiments.

Conclusions: Theoretical studies indicate that a complete breaking of NO bond is not necessary for CO to combine with an O atom. A 10% vibrational stretch of NO is sufficient for CO_2 formation over a substantially reduced barrier. Investigations also indicate that the N atom attached to the metal site reacts with the oncoming NO to form N_2O as an intermediate.

Infrared Spectroscopy of CO Oxidation by a Cobalt-Based Oxide Catalyst

Piers Newbery[1], John B. Paine[1], Benjamin A. Weinstock[2], Matthew J. Pollard[2], Husheng Yang[2], and Peter R. Griffiths[2]
[1]Philip Morris USA, Richmond, Virginia
[2]Department of Chemistry, University of Idaho, Moscow, Idaho

Hypothesis: Cobalt-based oxides, have been shown to act as room temperature catalysts for the oxidation of CO to CO_2, and thus have the potential to remove carbon monoxide from tobacco smoke when incorporated into a cigarette filter. However, exposure to the atmosphere and/or carbon monoxide can lead to excessive deactivation, whereby the catalyst needs heating well above room temperature to regain activity. Infra-red spectroscopic techniques and differential scanning calorimetry (DSC) have been used to investigate the mechanism(s) of catalysis and deactivation.

Results:
In situ diffuse reflection (DR) infrared spectra, during both catalyst activation by calcination and catalytic oxidation, demonstrated that under certain conditions a single CO molecule was adsorbed onto a metal ion, as evidenced by a band at 2006 cm^{-1}. Under different conditions, especially when the catalyst had been deactivated, DR spectra demonstrated the geminal substitution of two CO molecules onto a single highly oxidized metal ion and the physisorption of CO_2 onto an unidentified site.

An ultra-rapid scanning infra-red spectroscopic instrument was used to look at gas mixtures passed through a fast solenoid valve, through the catalyst, and into a long-path length, low-volume gas cell. A significant amount of the CO_2 that was formed appeared to be in a vibrationally excited state. This may be the first evidence of a vibrationally excited product resulting from a heterogeneously catalyzed reaction.

During CO oxidation, the temperature that the catalyst is allowed to reach determines the amount of deactivation. If the catalyst temperature remains low, then there is rapid deactivation. But if the heat from the exothermic oxidation reaction is used to increase the temperature of the catalyst bed, then the amount of deactivation can be reduced so that the reaction can continue indefinitely.

Conclusions:
The formation of vibrationally excited CO_2 suggests that the catalytic mechanism of the oxidation of carbon monoxide on these cobalt-based oxides may take place via a peroxide intermediate. Evidence has been obtained that carbon monoxide by itself can act to deactivate the catalyst, although the presence of water and/or oxygen are also very important in determining the catalytic process. Heat from the CO oxidation reaction can be used to prevent deactivation of the catalyst during use.

SCF-Assisted Microencapsulation Studies

Mark A. McHugh[1], Zhihao Shen [1], Dan Li [1], and Georgios D. Karles[2]
[1]Department of Chemical Engineering, Virginia Commonwealth University, Richmond, Virginia
[2]Philip Morris USA, Richmond, Virginia.

Hypothesis: The objective of these studies is to determine experimentally the underlying physics and chemistry controlling the quality and performance of encapsulated materials consisting of flavor compounds surrounded by a polymeric coating created using supercritical fluid-assisted technology. Special emphasis is given to supercritical CO_2 for these studies. Fundamental kinetic information is also being determined using a novel spectro-turbidity technique that uses a pressure quench as opposed to a temperature quench to precipitate the microencapsulated material as a phase boundary is crossed. A key feature of the work proposed here is a thorough investigation of the phase behavior of the flavor compounds and the coating materials in a variety of SCF solvents at conditions covering wide ranges of pressures and temperatures.

Results: At present the phase behavior has been determined for a family of pyrazines, including pyrazine, 2-methyl pyrazine, 2-acetyl pyrazine, 2-methoxy-pyrazine, and 2,3 pyrazine, in CO_2. These materials are highly soluble in CO_2 at very low pressures and temperatures as shown in Figure 1 for the 2-methoxy-pyrazine system. Hence, it is viable to encapsulate pyrazine into a polymer host at pressures well below 2,000 psia and at temperatures near 40 to 50 °C. Current work is demonstrating the CO_2-assisted encapsulation technique using a variety of candidate polymers including poly(ethylene-co-vinyl acetate), an FDA-approved material for polymeric drug delivery devices. The encapsulated materials are created using a pressure-quench technique as well as a ball milling technique, both in the presence of an SCF solvent.

Conclusions: In this talk we describe the fundamental chemistry and physics underlying the SCF-assisted encapsulation of flavors in polymeric host materials. Data are presented for a variety of pyrazines in CO_2 and this information is integrated into an experimental protocol developed for forming microencapsulated materials. Preliminary encapsulation results will be reported in this talk.

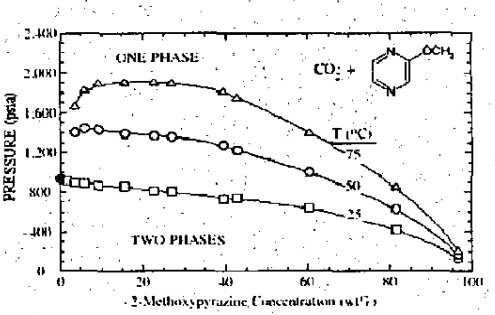

Figure 1. Phase behavior of 2-methoxy-pyrazine in CO_2 obtained in this study.

Poster Session

Fifth Philip Morris USA Symposium on Fundamental Science

Jefferson Hotel
Richmond, Virginia
October 28-30, 2003

Poster Session		
Tuesday, October 28, 2003		
Chair: Weijun Zhang		
1-1	Cigarette Smoke-Induced Endothelial Dysfunction in vitro: Role of the Cyclooxygenase Pathway	**K. von Holt**, S. Lebrun, R. Schleef
1-2	Gene Expression Profiling in Respiratory Tract Tissues of Rats Following Exposure to Mainstream Cigarette Smoke	S. Gebel, B. Gerstmayer, A. Bosio, E. Van Miert, **T. Müller**
1-3	A Population Pharmacokinetic Model for Nicotine as a Biomarker of Smoke Exposure	M. Gogova, **H. J. Roethig**, D. Mould, and M Sarkar
1-4	Cigarette Parameters that Influence the Mutagenicity of Mainstream Smoke Condensate	F. J. Tewes, T. J. Meisgen, W. A. Gomm, **E. Roemer,** and R. A. Carchman
1-5	Assessment of ETS Exposure among Non-Smokers using Biomarkers and a Questionnaire	**R. W. Lau,** M. Zhang, J. Oey, Y. Jin, and R.-A. Walk
1-6	3-Aminobiphenyl and 4-Aminobiphenyl Hemoglobin Adducts in Adult Smokers and Non-Smokers	**Mohamadi Sarkar**, Roger Walk, Regina Stabbert, Robin Kinser, and Hans Roethig
1-7	Evaluation of Cigarette Smoke-Induced Intermediate Chronic Obstructive Pulmonary Disease (COPD) Biomarker Responses in Mice	**C. J. Obot**, K. M. Lee, A. F. Fuciarelli, R. B. Westerberg, and W. J. McKinney
1-8	Relationships Between Tobacco Filler Levels of TSNA and Mainstream Smoke TSNA	**Susan Tafur** and David Rockwell
1-9	XAFS Study on the Oxidation State of Palladium Acetate on Cellulose as a Function of Temperature	**Shaheen Islam**, Thomas McGrath, and Don Miser
1-10	Effects of Certain Solids and Gas-Phase Species on the Formation and Growth of PAH from Catechol Pyrolysis	**M. J. Wornat**, E. B. Ledesma, and S. Thomas
1-11	High Resolution TEM observation of salt-loaded cellulose chars	**W. Z. Zhu**, D. E. Miser, W. G. Chan, and M. R. Hajaligol

Fifth Philip Morris USA Symposium on Fundamental Science

Jefferson Hotel
Richmond, Virginia
October 28-30, 2003

1-12	Development of a Micro-Pellet Reactor to Aid in the Detection of Reactive Intermediates from and Characterization of Biomass char by Laser Pyrolysis MBMS	**Joshua Lee**, J. Thomas McKinnon, Andrew M. Herring, David Petrick, Bryan D. McClosky, Ryan A. Pavelka, and Matthew Kirchner
1-13	Heat Balance in the Burning Cigarette	**Bruce Waymack**, Joseph Banyasz and Kenneth Shafer
1-14	A Modeling Analysis of Non-Melting Solid Fuel Particle Heating	**Ali A. Rostami**, Susan E. Wrenn, and Mohammad R. Hajaligol
1-15	A Thermophysical Model of Steady-Draw Cigarette Combustion	**Sung Yi**, M. Subbiah, F. Rasouli, and Peter J. Lipowicz
1-16	A Comprehensive Model of Electrically Heated Smoking System	**Sung Yi**, M. Subbiah, F. Yang, and S. Wrenn
1-17	Morphological Characterization of Component Tobaccos	**Vicki L. Baliga**, Michael E. Thurston, W. Geoffrey Chan, and Mohammad R. Hajaligol
1-18	Temperature Dependence of Radical Formation from Hydroquinone and Catechol	**Lavrent Khachatryan**, Hiue Truong, Lacramioara Negureanu, Randall Hall, and Barry Dellinger
1-19	Development of Monitoring Techniques for Hydrogen Peroxide Related to Exposure to Cigarette Smoke	**F. Yan**, R. Jagannathan, G.D. Griffin, C. J. Brown, D. L. Stokes, A. L. Wintenberg, and T. Vo-Dinh
1-20	Effect of Oxygen on the Characteristics of Bright tobacco char	**W.Z. Zhu**, W. Geoffrey Chan, and Mohammad R. Hajaligol

Wednesday, October 29, 2003

Chair: Zhaohua Luan

2-1	Development of an FT-IR Spectrometer – 5-Port Smoking Machine Instrument for Rapid Quantitative Analysis of Gas Phase Constituents in Cigarette Smoke	**Susan Plunkett** and David Self
2-2	Rapid Screening Methods for Smoke Constituents in Mainstream Smoke	**C. B. Huang** and David Self
2-3	A Real-time GC/MS method for Puff by Puff Analysis of Whole Smoke	**I. Skinner**, D. S. Kellogg, H. Yu , and Ric Brower
2-4	Influence of Preheating Tobacco on the Yields of Smoke Products	**Wei-Jun Zhang**, Mohammad S. Rostami, and Firooz Rasouli

Fifth Philip Morris USA Symposium on Fundamental Science

Jefferson Hotel
Richmond, Virginia
October 28-30, 2003

2-5	Determination of Molecular Parameters for Quantitation of non-HITRAN Molecules using Lead-Salt TDL-IR	**Charles N. Harward**, Randall E. Baren, and Milton E. Parrish
2-6	Formation Mechanisms of Nitrogenous Char and NO during Biomass Oxidation	**Hoongsun Im**, Firooz Rasouli, Mohammad R. Hajaligol
2-7	Role of Tobacco Solanesol in PAH Formation	**Thomas E. McGrath**, Gail Yoss, Jan B. Wooten and W. Geoffrey Chan
2-8	Phenolic Compound Formation from Tobacco and Tobacco Components	Gayle M. Powers, **Raquel M. Olegario**, Thomas E. McGrath, and W. Geoffrey Chan
2-9	Tunable Laser System fro Single Particle Mass Spectrometry	**Ramkuber Yadav**, Joseph Banyasz, Mohammad Hajaligol
2-10	Reentrainment of Submicron Solid Particles from Inside Cylindrical Surfaces	**Ramin Mortazavi**, Timothy Cameron, James McLeskey, and Mohammad Hajaligol
2-11	Performance of an Aerosol Sampling and Dilution System	**Ali Rostami**, Steven Larson, and Sue Wrenn
2-12	A Parametric Study of Transport of Aerosol Particles in a Heterogeneous Shredded Porous Media	M.S. Saidi, **K. Shafer**, and P. Lipowicz
2-13	Correlation of Gas Phase Products with Char Composition Resulting from Maillard Chemistry	**Bob Evans**, Thomas Sherow, Karl Andreason, Mike Looker, Mark Nimlos, and Luc Moens
2-14	Synthesis and Characterization of Nanocrystalline Cu/CeO2 catalyst for CO Oxidation by Laser Vaporization and Controlled Condensation Method	**R. S. Sundar**, S. Deevi, and D. Miser
2-15	Commercially available color pigments as potential candidates for CO oxidation catalyst	**S. Gedevanishvili**, S. PalDey, and F. Rasouli
2-16	Effect of Changes in Crystalline Phases and Microstructure on the CO oxidation Activity of Pd/ZnO-based Catalysts	**Yezdi B. Pithawalla**, Rangaraj S. Sundar, Jan A. Lipscomb, and Sarojini Deevi
2-17	Thermal Reaction of Catechol over Nanoparticle Iron Oxide and Quartz	**Eun-Jae Shin**, Mohammad R. Hajaligol, W. Geoffrey Chan, and Firooz Rasouli
2-18	A Comparison of Menthol Delivery from two Menthol Release Agents and their Thermal Properties	**Kathryne Esperdy**

Cigarette Smoke-Induced Endothelial Dysfunction in vitro: Role of the Cyclooxygenase Pathway

K. von Holt, S. Lebrun, R. Schleef
PHILIP MORRIS Research Laboratories GmbH, Cologne, Germany

Endothelial dysfunction is hypothesized to be a key mechanism by which cigarette smoke promotes vascular disease. Although animal assays for endothelial dysfuncton routinely investigate the vasodilatory properties of aortic rings *in vitro*, information is limited on the ability of these vessels to function in the presence of tobacco smoke. In this study, we examined the effect of cigarette mainstream smoke (MS) on the contraction and relaxation of rat aortic rings *in vitro*. Thoracic aortas were prepared from euthanized male Wistar rats and aortic rings were suspended in Krebs buffered saline in organ bath chambers. MS from 2R4F reference cigarettes was generated on a 30-port smoking machine and bubbled through phosphate buffered saline (PBS) and used within 30 minutes. Incubation of aortic rings for up to 60 minutes with smoke-bubbled (SB)-PBS (≤0.06 puff/ml) had no effect on norepinephrine-induced contraction; however, relaxation of the rings in response to acetylcholine (Ach; 10^{-8} - 10^{-4} M) was reduced in a dose-dependent manner. For example, relaxation of norepinephrine-contracted aortic rings, which were pre-incubated *in vitro* for 45 minutes with 0.06 puff/ml SB-PBS, was 16.8 ± 11.9% at 10^{-4} M Ach compared to 96.3 ± 6.4% relaxation for control rings ($P<0.001$; n=6). The MS-inhibition of Ach-induced relaxation was reversible and normal contraction/relaxation curves could be obtained following washing to remove the SB-PBS and/or vaso-active reaction products. MS-inhibition of Ach-mediated relaxation appeared to be mediated by a cyclooxygenase-dependent pathway because indomethacin (10 uM) was effective in normalizing the Ach-relaxation curves to levels observed for controls incubated in the presence of indomethacin ($p<0.01$, n=6). These data indicate that the incubation of aqueous preparations of MS with rat aorta *in vitro* result in the generation of a cyclooxygenase-dependent vasoconstrictor and raise the possibility that this pathway may play a role in the vasoconstricting effects of MS within certain regions of the circulatory system.

Gene Expression Profiling in Respiratory Tract Tissues of Rats Following Exposure to Mainstream Cigarette Smoke

S. Gebel[1], B. Gerstmayer[2], A. Bosio[2], E. Van Miert[3], **T. Müller**[1]
[1]PHILIP MORRIS Research Laboratories GmbH, Köln, Germany
[2]Memorec Stoffel GmbH, Köln, Germany
[3]CRC Contract Research Center, Zaventem, Belgium

There is strong evidence that cigarette smoking is associated with the development of cancer, cardiovascular disease, and chronic obstructive pulmonary disease. However knowledge is fragmentary regarding global changes in gene expression patterns in the target tissues exposed to cigarette smoke (CS).

To expand this knowledge, gene expression patterns were investigated in Sprague Dawley rats exposed to CS (100 µg tobacco particulate matter/l): single exposure of 3 h or multiple exposures of 3 h/day, 5 d/week for 3 weeks with sacrifice immediately after exposure or 24 h after exposure. RNA was prepared from rat nasal respiratory epithelium (RNE), trachea, and lung tissue. Gene expression profiling was done using microarrays carrying 2032 cDNA probes.

The strongest differential gene expression was seen in RNE after 3 h, with a pronounced up-regulation of oxidative stress-related genes (e.g., *heme oxygenase-1 (HO-1)*: 52x; *NADPH-quinone-oxidoreductase*: 20x; *γ-glutamylcysteine-synthetase* 7x) and genes encoding xenobiotic metabolizing enzymes (e.g., *cytochromeP4501A1:* 140x, *aldehyde dehydrogenase-3*: 31x). After 3 weeks, the strength of induction of these oxidative stress-response genes was significantly decreased (down to 28% for *HO-1* expression) pointing to an adaptive response which was also seen overall: 57 genes were induced after 3 hours of exposure (> 2-fold) compared to only 22 genes induced after 3 weeks of exposure. In contrast, the induction of *cytochromeP4501A1* and *aldehyde dehydrogenase-3*, assumed to be regulated via AHR-activation, was not reduced after 3 weeks of exposure.

Compared to RNE, results from lung tissues showed a broader gene induction after 3 weeks than after 3 h (24 genes versus 7). This, along with the overall lower response in the lung, might be attributable to a deposition gradient of oxidative stress-inducing components from the upper to the lower respiratory tract. Conversely, the induction of *cytochromeP4501A1* was similarly high in the lung and RNE independent of the exposure time.

Gene expression patterns in rats which were allowed to recover for 24 hours after exposure showed that nearly all changes observed immediately after exposure had reversed to control levels, regardless of whether there was a single 3-h exposure or multiple exposures over 3 weeks. This indicates that exposure over 3 weeks did not induce persistent alterations in gene expression.

This study shows differential gene expression analysis in tissues from CS-exposed animals to be a highly sensitive tool to detect specific stress responses prior to the onset of inflammatory and/or morphological changes. Further studies are required to verify whether these changes in expression profiles are the first hints of a long-term effect leading to CS-related diseases.

A Population Pharmacokinetic Model for Nicotine as a Biomarker of Smoke Exposure

M. Gogova[1], H. J. Roethig[1], D. Mould[2], and M Sarkar[1]
[1] Philip Morris USA, Richmond, Virginia
[2] Projections Research Inc., Phoenixville, Pennsylvania

Objective: To develop a population pharmacokinetic model for nicotine to determine the inter-subject variability and population exposure in adult smokers using conventional lit-end (CC) and electrically heated cigarette smoking system (EHCSS).

Subjects and Methods: Nicotine equivalents (NE, molar sum of nicotine and its glucuronide, cotinine and its glucuronide, *trans*-3'-OH cotinine and its glucuronide) were measured in 24 hr urine samples from adult smokers smoking CC (n=40), or EHCSS (n=40) or stop smoking (n=30). 433 NE observations from 110 subjects were analyzed using NONMEM (Version V). The PK model was a 1 compartment open model with 0 order input and 1st order elimination and parameterized for clearance (CL/F), volume of distribution (Vd/F) and bioavailable fraction F of NE. Covariates such as number of cigarettes (ncig), fraction of cigarette smoked, cigarette type, FTC tar delivery were tested for influence on F of NE. Additional covariates such as age, gender, race, weight, serum creatinine, creatinine clearance, BMI, liver function, were evaluated to explain population parameter variance.

Results: The estimated mean (%CV) for CL=0.24 (31)L/min, Vd =7.87 (32)L and t1/2 for NE was 22.35 hr. Inter-subject variability in clearance was reduced from 93% to 31.7% by adding ncig, FTC tar delivery, cigarette type, gender effect into model. The relative dose of NE was positively correlated with ncig, FTC, and cigarette type and changed by a factor of 1.5 in CC compared to EHCSS smokers. Of the additional covariates evaluated, only gender had a statistically significant effect on CL/F. The proportional residual error (PRE) was 23%, and additive residual error was 0.03

Conclusion: The model predicts the population exposure to nicotine for different cigarette types and different FTC tar delivery. Most inter-subject variability was explained by ncig, FTC, cigarette type and subject gender.

Cigarette Parameters that Influence the Mutagenicity of Mainstream Smoke Condensate

F.J. Tewes, T.J. Meisgen, W.A. Gomm, **E. Roemer,** and R.A. Carchman
PHILIP MORRIS Research Laboratories GmbH, Cologne, Germany

The Salmonella reverse mutation assay has been used to determine the influence of various cigarette design parameters on the mutagenicity of mainstream smoke condensate. Cigarette prototypes that differ in blend composition, paper porosity, paper additive (citrate or phosphate), filtration efficiency, and filter ventilation were constructed. In a fractional, factorial study design, 30 cigarette types were selected form 486 possible combinations. Three levels of each parameter were represented by 10 different cigarette types. Cigarettes were smoked according to ISO standards, and 4 condensate batches per type were collected by impaction and dissolved in dimethyl sulfoxide. Mutagenicity determination was carried out in the plate incorporation version of the Ames assay with *S. typhimurium* strain TA98 in the presence of S9. Four equidistant doses from 0.04 to 0.16 mg dry condensate per plate were applied. The specific mutagenicity, i.e., revertants/mg dry condensate, of each batch was calculated using linear regression analysis with Poisson-weighted data. To determine the influence of the cigarette design parameters, a multiple linear regression analysis on the specific mutagenicity values was performed. All regression coefficients except those for the paper additives were statistically significant ($p < 0.001$). Increasing the amount of Burley for bright tobacco from 0% to 65% resulted in a 2.4-fold increase; filter ventilation from 5% to 60%, in a 1.2-fold increase; filtration efficiency from 35% to 55%, in a 1.1-fold increase; and paper porosity from 10 cm/min to 45 cm/min, in a 0.89-fold decrease in specific mutagenicity.

Assessment of Eenvironmental Tobacco Smoke (ETS) Exposure Among Non-Smokers using Biomarkers and a Questionnaire

R. W. Lau, M. Zhang, J. Oey, Y. Jin, and R.-A. Walk
Philip Morris USA, Richmond, Virginia

<Abstract Not Available>

3-Aminobiphenyl and 4-Aminophenyl Hemoglobin Adducts in Adult Smokers and Nonsmokers Phenotyped for CYP1A2 and NAT2 Activity

Mohamadi Sarkar, Roger Walk, Regina Stabbert, Robin Kinser, and Hans Roethig
Philip Morris USA, Richmond, Virginia

Aromatic amines found in cigarette (cigt) smoke and other sources have been suggested to be carcinogenic due to activation of the N-hydroxyl metabolites formed by CYP1A2. Hemoglobin adducts of 3-aminobiphenyl (3-ABP Hb) and/or 4-aminobiphenyl (4-ABP Hb) may be used to monitor cigt smoke exposure. It has been suggested that 3-ABP Hb is a more specific biomarker of cigt smoke exposure. Slow acetylators have been found to exhibit higher amounts of the Hb adducts due to inefficient acetylation. The goal of this study was to determine the role of CYP1A2 and NAT2 phenotype on 3-ABP and 4-ABP Hb adducts and to determine the intra- and inter-individual variability in the adduct levels. The study was conducted in adult smokers (S, n=72) smoking at least one cigt (3-6.9 mg FTC tar range) every day for over the last 12 months, and nonsmokers (NS, n=68). The subjects were phenotyped for CYP1A2 and NAT2 using urinary caffeine metabolites. Blood samples were collected to measure levels of 3-ABP Hb and 4-ABP Hb twice within 6 weeks (wk) by capillary GC-MS. The CYP1A2 activity [ratio of (1,7-methyluric acid + 1,7-dimethylxanthine)/(1,3,7-trimethylxanthine)] was higher ($p<0.001$) in S (6.8 $\pm$3.71) compared to NS (4.07 $\pm$2.59). A bimodal distribution was observed for the NAT2 activity [(5-acetylamino-6-formylamino-3-methyluracil, AFMU)/ (1-methylxanthine)] indicating slow and fast acetylators. No differences were observed in NAT2 activity, between S and NS. The levels of 4-ABP Hb adducts were significantly ($p<0.0001$) greater in S (32.4 $\pm$17.8 pg/g Hb) compared to NS (7.8$\pm$4.9 pg/g Hb). The levels of 3-ABP Hb adducts (3.4 $\pm$3 pg/g Hb) while significantly greater ($p<0.05$) in S compared to NS were about 10-fold lower in S compared to 4-ABP Hb adducts in the same group. There was no difference in both the adduct values when compared between the two weekly measurements for the same individuals. Intra-individual variability (%CV) obtained by comparing Hb adduct levels from wk 1 to wk 6 was ~23% for 3-ABP and ~19% for 4-ABP Hb adducts. Significant correlation ($p<0.001$) was observed for both 3-ABP and 4-ABP Hb adducts with number of cigts smoked. Evaluation of the relationship between 3-ABP and 4-ABP Hb adducts ($r^2=0.69$) suggests that the exposure to one or both aromatic amines is from other sources in addition to cigts. The levels of 4-ABP Hb adducts appeared to increase with CYP1A2 activity ($r^2=0.20$) whereas this relationship was much weaker with the 3-ABP Hb adducts ($r^2=0.06$). The lack of correlation between the Hb adducts in slow and fast acetylators, suggest that acetylator phenotype has no influence on ABP Hb adducts. Although there appears to be less confounding factors in the measurement of 3-ABP Hb adducts in nonsmokers, its utility as a biomarker of exposure to cigarette smoke is limited due to the low levels observed in smokers. The lack of significant differences between measurements taken on week 1 compared to week 6 suggests that a single blood sample would be adequate to monitor current exposure.

Evaluation of Cigarette Smoke-Induced Intermediate Chronic Obstructive Pulmonary Disease (COPD) Biomarker Responses in Mice

C. J. Obot[1], K. M. Lee[2], A. F. Fuciarelli[2], R. B. Westerberg[2], and W. J. McKinney[1]
[1]Philip Morris USA, Richmond, Virginia
[2]Battelle Toxicology Northwest, Richland, Washington

Recent studies suggest that C57BL/6 (C57) mice develop emphysema following chronic cigarette smoke exposure while ICR mice do not. In this study, these two strains of mice were used to investigate subacute cigarette smoke exposure-related changes in intermediate biomarkers of COPD. Male C57 and ICR mice received a 2-hr nose-only exposure to mainstream cigarette smoke of 2R4F cigarettes (75, 250 and 600 µg TPM/L) or filtered air for 7 consecutive days. BAL fluid samples were collected at 2 and 12 hrs post-exposure and analyzed for LDH, NAG, protein, cell differentials, apoptosis, cytokines [KC (IL-8), TNF-α, IFN-γ, IL-1β, IL-5, IL-6, IL-10, IL-13, IL-17, GM-CSF, JE, MIP-1α, MIP-2, RANTES, TARC, SDF-1β], and GSH/GSSG. At 0-hr post-exposure, blood samples were analyzed for biomarkers of exposure (COHb and nicotine). In addition, the respiratory tract was microscopically examined. Exposure biomarkers were slightly greater in the C57 compared to the ICR. More necrosis was observed in the nasal epithelium of exposed C57. Apoptosis was increased in cells recovered from ICR mice at 600µg/L TPM. Overall, exposure-related increases in cytokines and neutrophil counts were greater in ICR mice. However, some cytokines (TARC, 1β) and NAG (a marker of cellular necrosis) were greater in C57 groups at 250µg/L TPM. These results suggest that cellular responses to subacute cigarette smoke exposures (e.g. apoptosis and/or necrosis) may be early indicators of COPD. Therefore specific cytokines, markers for apoptosis and/or necrosis, and BAL cell differentials may serve as intermediate biomarkers of COPD in a mouse model that can be used in the evaluation of smoking products designed to reduce exposure to toxic constituents.

Relationships Between Tobacco Filler Levels of Tobacco Specific Nitrosamines (TSNA) and Mainstream Smoke TSNA

Susan Tafur and David Rockwell
Philip Morris USA, Richmond, Virginia

Levels of mainstream smoke (MS) TSNA from tobacco blends containing reduced TSNA tobaccos are influenced by a number of factors. Blend components differ in puff count and the amount of tobacco burned per puff which in turn affects the total tar and TSNA delivery from a blend. Consequently, MS tar and TSNA deliveries are not simple additive functions based on individual component weight percentages in blends. In addition, there can be substantial differences in filler TSNA levels based on stalk position, geographical source of origin, cultural practices, and seasonal variation within specific tobacco types. Different reconstituted tobacco materials in blends can also complicate the relationships between filler and smoke TSNA.

Examples of correlations between TSNA in tobacco components and blends and smoke TSNA will be described. These relationships along with a database of filler levels of TSNA in numerous tobaccos, tobacco materials and by-products have been used to develop a model to estimate the impact on MS TSNA of inclusion of reduced TSNA tobaccos into blends.

XAFS Study on the Oxidation State of Palladium Acetate on Cellulose as a Function of Temperature

Shaheen Islam[1], Thomas McGrath[2] and Don Miser[2]
[1]Virginia Union University, Richmond, Virginia
[2] Philip Morris USA, Richmond, Virginia

Hypothesis: X-ray Absorption Fine Structure (XAFS) has been used as a complementary technique to study the catalytic effect of metal on the thermal decomposition of Avicel cellulose as a function of temperature. XAFS is the ideal tool for characterization of catalysts and related materials. A great advantage of XAFS in relation to catalyst characterization is the ability to perform experiment under realistic condition.

Results: Microcrystalline cellulose powder containing 1 w/w% of metal was prepared using $Pd(OOCCH_3)_2$ as metal source. The samples were pyrolyzed isothermally in helium, for 10 minutes, at temperatures ranging from 150°C to 600°C. The gas chromatography (GC), coupled with mass spectrometry (MS), was used to analyze the condensable volatiles (tar). The GC/MS analysis indicated changes in chemical composition of tar due to the presence of metal. The XAFS spectra were collected at Pd k-edge for the fresh, unpyrolyzed, samples and for the solid residues (chars) obtained after the thermal treatment. The data were taken at transmission mode, at National Synchrotron Light Source (NSLS), using beam line X11A. The unpyrolyzed cellulose-metal acetate samples demonstrated oxygen as nearest neighbors to metal, since the acetate portion of the salt remained intact. After fitting the data with standard, we found Pd-O distances in the range of 1.973-2.014Å. High Resolution Transmission Electron Microscope (HRTEM) had been used to study the morphology of the charred samples, which indicated the presence of a relatively uniform particle size distribution in the low nanometer range.

Conclusion: Pure $Pd(OOCCH_3)_2$ undergoes thermal decomposition, in helium, between 150°C and 200°C. However, The local structure remains relatively unchanged over the range of 200°C to 400°C. The preliminary XAFS result of the charred samples has indicated that the palladium is completely reduced to its metallic state at 600oC, which is consistent with the results, obtained using other techniques.

The Effects of Certain Solids and Gas-Phase Species on the Formation and Growth of PAH from Catechol Pyrolysis

M. J. Wornat, E. B. Ledesma, and S. Thomas
Louisiana State University, Department of Chemical Engineering,
Baton Rouge, Louisiana

Hypothesis: Within the context of a burning cigarette, the presence of certain solids (*e.g.*, $CaCO_3$, Fe_2O_3, NH_4MgPO_4, and char) and of certain gases (*e.g.*, O_2, NH_3, and C_1 to C_4 hydrocarbons) may influence the formation and growth of PAH. Insight into any PAH-promoting or PAH-inhibiting effects of each of these substances can be gained from pyrolysis experiments with catechol, conducted both in the absence and in the presence of each of these solids and gas-phase species.

Results: Yielding detailed PAH product speciation and yields, our previous catechol pyrolysis experiments have all been conducted in the gas phase, in nitrogen, and at temperatures of 500 to 1000 °C. Three new sets of catechol pyrolysis experiments, at temperatures in the range of 300 to 900 °C, are planned. In the first set, catechol will be pyrolyzed in separate experiments with each of the following solids: $CaCO_3$, Fe_2O_3, NH_4MgPO_4, and char. The products from these heterogeneous experiments will be collected and analyzed for comparison with the catechol product distributions from the homogeneous experiments. In the second set of experiments, catechol will be pyrolyzed in nitrogen that is doped, in separate experiments, with each of the following gases: O_2, NH_3, and certain C_1 to C_4 hydrocarbons thought to be key participants in PAH ring-growth reactions. The third set of catechol pyrolysis experiments will be conducted in the presence of selected pairings of solids with added gases.

Conclusions: The above planned experiments should lead to an assessment of the effects of certain solids and gases—some naturally present in a burning cigarette; others purposely added to reduce other byproducts—on PAH formation and growth in the context of a burning cigarette.

High Resolution Transmission Electron Microscope Observation of Salt-Loaded Cellulose Chars

W. Z. Zhu, Donald E. Miser, W. Geoffrey Chan, and Mohammad R. Hajaligol
Philip Morris USA, Richmond, Virginia

Hypothesis: It has been documented that addition of palladium acetate at a concentration of 1wt% into cellulose brings about noticeable drop in the yield of polycyclic aromatic hydrocarbons (PAHs) during pyrolysis, in particular, large ring PAHs, whereas the incorporation of potassium acetate exhibits the opposite effect. High resolution transmission electron microscope (HRTEM) is a viable tool to provide deeper insight into the underlying mechanisms and direction for our ongoing effort in identifying potential palladium alternative.

Results:

1. For palladium-containing material: significant aggregation of palladium black particles, with size in the range of several submicrometers, was observed as palladium is physically mixed with cellulose matrix. Most of the particles have been oxidized as confirmed by Fast Fourier Transform (FFT) although zero valence particles can still be found. Palladium particles were revealed to be embedded within the cellulose char for the PdOAc-bearing samples that have been pyrolyzed with fast heating rate. Particles are uniformly dispersed and largely absent of aggregates with average size below 5nm. Overwhelming majority of particles has undergone reduction reaction into palladium metals in the course of pyrolysis despite the presence of remnant oxidized particles. Samples subjected to sluggish heating during pyrolysis saw substantial growth and impingement of particles whose size approaches as large as 50nm, in sharp contrast to the samples with slow heating. Predominant amount of particles are present in the form of palladium metals. This observation indicates that particle size plays a crucial role in determining the catalytic activity of the palladium.
2. For potassium-containing material: No potassium particles or crystallites were observed in the unpyrolyzed KOAc-containing material, suggesting the dissolution or diffusion of metal species into cellulose matrix. Upon increasing the pyrolysis temperature, potassium displays a strong tendency of migration to form potassium-rich regions that are of somewhat intermediate structure between amorphous and crystalline structure. EDS results clearly show that potassium within the matrix is progressively depleted, rather than eliminated, as the pyrolysis temperature is increasingly raised.

Conclusions: The sharply different roles found for palladium acetate and potassium acetate loaded cellulose in impacting the PAHs yield during pyrolysis can be, at least partially, traced to the significantly different morphologies and distributions of the metallic particles within the cellulose matrix. Presence of uniform and nano-sized particles appears to be one of key factors in preserving the desired catalytic activity.

The Development of a Micro-pellet Reactor to Aid in the Detection of Reactive Intermediates from and Characterization of Biomass Char by Laser Pyrolysis Molecular Beam Mass Spectroscopy

Joshua Lee, J. Thomas McKinnon, Andrew M. Herring, David Petrick, Bryan D. McClosky, Ryan A. Pavelka, and Matthew Kirchner
Department of Chemical Engineering, Colorado School of Mines, Golden, Colorado

Hypothesis: That accurate temperatures can be modeled for charring and pyrolysis in a micro-pellet device in which the substrate is smaller than the laser beam diameter. In addition that we will be able to apply a laser heating profile such that charring and pyrolysis conditions of actual cigarette smoldering and puffing can be reproduced.

Results:

- Laser Pyrolysis of biomass has proved to be an extremely valuable tool for the detection of reactive intermediates produced when biomass is rapidly heated, but it is difficult to measure the temperature of the lased substrate directly. In the experiments performed by us to date the large sample relative to the laser spot size has also made temperature estimates by modeling inaccurate.
- A first generation micro-pellet reactor design was built, and was used to collect proof of concept data. However, this reactor only allows the sampling of 12 micro-pellets, a number insufficient to give sufficient signal to noise ratios to detect the large PAH and PAC of interest. This design also resulted in some uneven charring of the test cellulose pellets.
- A second generation reactor design is currently being tested, and thus far has shown even charring.

Conclusions: We hope to increase the signal to noise ratios by increasing the number of micro-pellets held by the reactor and averaging out the background scans. This will be a necessary step to detect PAH and PAC larger than about m/z 202. We will eventually mimic the temperature profile observed during cigarette smoking and observe the reactive intermediates produced by MBMS.

Heat Balance in the Burning Cigarette

Bruce Waymack, Joseph Banyasz and Kenneth Shafer
Philip Morris USA, Richmond, Virginia

Hypothesis: The self-sustaining smoldering cigarette is a delicate balance between heat generated by oxidation reactions and heat loss by various means. This intricate network of processes can be evaluated and explained in terms of measured and calculated parameters.

Results: From previous work we have established that, during free smolder, the heat output of a conventional cigarette is proportional to the mass burn rate (MBR) of the tobacco rod; that the coal size and rate of oxygen consumption are also proportional to MBR; and that the heat of smoldering combustion is a constant independent of conventional cigarette design parameters. The coal surface temperature and heat flux are approximately constant as well. The heat of combustion for free smolder is only about half that of complete combustion of tobacco.

We have since shown that the heat output is much higher during a puff, but the net heat generated per gram of tobacco during puffing is significantly less than during free smolder. The heat output varies proportional to the flow rate during a puff. The quantity of heat that can be removed from the smoldering cigarette coal that will lead to extinguishment is roughly 10 % of the total heat produced. This is because the heat required, per gram, to bring the tobacco bed to a state of self-sustaining oxidation is about 10 % of the heat generated per gram of tobacco during smoldering. The internal maximum coal temperature during smolder is approximately constant until the MBR approaches the critical region of extinguishment (minimum MBR), where it drops to a minimum of about 600 °C. When a cigarette self-extinguishes, it does so in a near linear fashion with respect to burn rate and can be revived by puffing at burn rates below the minimum sustaining level.

Conclusions:

- The concept of reducing coal temperature in a conventional cigarette enough to significantly reduce aromatic pyrolysis products and still have the cigarette self-sustain smolder does not seem feasible.

- The smoldering cigarette is a delicate balance between heat generated by char oxidation reactions, heat needed to produce char, and heat lost to the environment. Measured and calculated parameters can account for the overall processes that are occurring.

A Modeling Analysis of Non-Melting Solid Fuel Particle Heating

Ali A. Rostami, Susan E. Wrenn and Mohammad R. Hajaligol
Philip Morris USA, Richmond, Virginia

Hypothesis: Heating of fuel particles is generally the first step in the process of gasification or combustion of solid fuels such as coal and biomass. The particle pyrolysis involves a series of complicating thermal effects including: internal convection, surface blowing effects, variation of solid thermal conductivity, and reaction heats. A numerical model was developed to investigate the effects of these factors on the eventual particle heating rate.

Method of Analysis: The equations of conservation of mass and energy including the above-mentioned effects were solved numerically for a shred. A simple first-order reaction model for the total weight loss was coupled with the transient thermal model. Thermal equilibrium between the solid and gas phase was assumed.

Results: The results show that internal convection tends to equalize the temperature distribution within the solid, while the blowing effect contributes to the boundary layer thickening and eventually to a reduction in the convection heat transfer to the particle from the surrounding gas. Heat of pyrolysis reactions plays an important role in the heating profile of the particle. It delays the temperature rise of the particle until most of the volatile materials are released.

A Thermophysical Model of Steady-Draw Cigarette Combustion

Sung Yi[1], M.Subbiah[2], F. Rasouli[2], and Peter J. Lipowicz[2],
[1]Department of Chemical Engineering, Hanyang University, Seoul, Korea
2Philip Morris USA, Richmond, Virginia

Hypothesis: The state of development of tobacco-structure-based submodels, computational hardware, and numerical algorithm has advanced sufficiently to allow development of an improved, computerized, steady-draw cigarette combustion model.

Results: The tobacco submodels that are based on structure included the functional group pyrolysis model which assumes that tobacco is composed of various chemical functional groups. The two-dimensional, unsteady, axisymmetric model developed in this work is the first comprehensive steady-draw cigarette combustion model to predict overall cigarette behavior. The model predicts functional group evolution and can be used to determine the length of the pyrolysis and combustion zones. Gaseous species, generated in evaporation, pyrolysis and combustion regions, may, because of pressure gradients be forced to flow towards both the unreacted solid and the already charred region. The continuity equation along with the momentum equations with reactive porous medium sink terms couple the external fluid flow with the gas flows generated in the tobacco bed due to gas evolution. Also, the peripheral air influx in front of the paper burn line was accurately predicted by treating the paper as a separate reactive porous medium entity from the tobacco rod.

Current advancements in computational hardware and an advanced numerical scheme built in the commercial computational fluid dynamics code, FLUENT using user-defined-functions (UDFs) made it possible to thoroughly evaluate the two-dimensional cigarette combustion model under continuous puffing condition.

Conclusions: The primary contribution of this work is the development of an improved comprehensive steady-draw cigarette combustion model that utilizes advanced chemistry submodels that depend upon tobacco structure. The pyrolysis submodel predicts 14 different functional groups evolution. Pyrolysis is not instantaneous, and volatile yield significantly affects the temperature profile and the location of the maximum temperature. Various dips and peaks in the temperature profile correspond to different functional groups that evolve different temperatures. Oxidation and gasification do not occur in separate zones. Also, gas phase chemistry is necessary to predict accurate species concentration profiles. Results suggest that solid-to-gas heat transfer for reacting tobacco beds is significantly smaller than for the non-reacting fixed-beds. Also, variable bed void fraction is necessary to predict accurate pressure drop in tobacco rods.

A Comprehensive Model of Electrically Heated Smoking System

Sung Yi[1], M. Subbiah[2], F. Yang[2], and S. Wrenn[2],
[1]Department of Chemical Engineering, Hanyang University, Seoul, Korea
[2]Philip Morris USA, Richmond, Virginia

Hypothesis: The state of development of tobacco-structure-based submodels, computational hardware, and numerical algorithm has advanced sufficiently to allow development of a comprehensive model of electrically heated smoking system.

Results: The tobacco submodels that are based on structure included the functional group pyrolysis model which assumes that tobacco is composed of various chemical functional groups. The three-dimensional, unsteady, model developed in this work is the first comprehensive novel smoking system, Accord, model to predict overall Accord behavior. The model predicts functional group evolution and can be used to determine the region of the pyrolysis in the tobacco mat upon electrically heating the heater blade. Gaseous species, generated in evaporation and pyrolysis regions inside the tobacco mat, may, because of pressure gradients be forced to flow towards both the unreacted solid and the already charred region. The continuity equation along with the momentum equations with reactive porous medium sink terms couple the external fluid flow with the gas flows generated in the tobacco mat due to gas evolution.

Current advancements in computational hardware and an advanced numerical scheme built in the commercial computational fluid dynamics code, FLUENT using user-defined-functions (UDFs) made it possible to thoroughly evaluate the three-dimensional novel smoking system, Accord, for a complete smoking cycle.

Conclusions: The primary contribution of this work is the development of a comprehensive Accord model that utilizes advanced chemistry submodels that depend upon tobacco mat structure. The pyrolysis submodel predicts 21 different functional groups evolution. Pyrolysis is not instantaneous, and volatile yield significantly affects the temperature profile. Various dips and peaks in the temperature profile correspond to different functional groups that evolve different temperatures. Evaporation of water do not occur in separate zones. Also, gas phase chemistry is necessary to predict accurate species concentration profiles. Results suggest that solid-to-gas heat transfer for reacting tobacco mat is significantly smaller than for the non-reacting fixed-beds. Also, variable bed void fraction is necessary to predict accurate pressure drop in tobacco mat. This model is a comprehensive multiphysics engineering tool can be used to study thermal-fluid-electrical-chemical behavior in a single environment.

Morphological Characterization of Component Tobaccos: Puff and Smolder Burn

Vicki L. Baliga, Michael E. Thurston*, W. Geoffrey Chan, Mohammad R. Hajaligol
Philip Morris USA, Richmond, Virginia

Hypothesis: Chemical components found in tobacco vary depending on the tobacco variety or the process used to make the product. Bright tobacco contains more reducing sugars and starch than Burley. Burley contains more soluble ammonia, nitrates, proteins, and ash than in Bright [1]. It might be expected that cigarettes made from different tobacco types exhibit unique morphologies.

Results: Cigarettes made from Bright, from expanded Bright, from Burley, and from Reconstituted Leaf were smoked through the fourth puff. For the smolder burn, the cigarettes were extinguished after the 4th puff. For the puff burn, the cigarettes were extinguished one sec into the 4th puff. The smoking regime used was 35 cc puff volume, 2 sec puff duration, and puffed once every 60 sec with a square wave puff profile.
All of the cigarettes made from the individual tobacco types exhibited similar morphologies during the smolder burn and similar morphologies during the puff burn. All tobacco types exhibited pooled cuticle melt, vesicle formation, and accumulations of K- and Cl-containing crystals on shreds under the char line. In the coal base region, much of the coal contained carbonized shreds often with inorganic crystals scattered across the epidermal surfaces. There were also regions within the coal that showed minimal heat damage. Areas next to the rod exterior showed extensive shred oxidation and ash formation. Shred morphologies were similar in the coal tip region to that of the coal base but more oxidized shreds were observed near the exterior and tip of the coal. During the puff burn, more variability in char morphology was observed. Channels of super-saturated, super-heated gases caused extensive vesicle formation, rapid crystal growth, and elongated rod/tube growth. Minor differences that were observed among the tobacco types included more rod/tube formations from Burley and from RL cigarettes.
Also measured were carbon, hydrogen, and nitrogen. More carbon was measured in the coal of Bright cigarettes than cigarettes made from Burley or RL. Burley, expanded Bright, and RL cigarettes lost more carbon in the smolder burn than the puff burn. The ash from cigarettes from all tobacco types showed a major loss of carbon and nitrogen. Hydrogen loss was more uniform from the coal base to the tip to the ash.

Conclusions: No unique shred morphologies were attributed to individual tobacco types. However, rod/tube growth seemed to be more prominent in Burley and RL puff burn cigarettes. More vesicle formation seemed to be associated with RL cigarettes. Carbon and nitrogen both tended to decrease very little in the cigarette coal but dropped precipitously in the ash. Hydrogen dropped in equal increments from the coal base to tip to ash. Tobacco from smolder burn cigarettes tended to lose more carbon and nitrogen while puff burn cigarettes tended to lose more hydrogen.

[1] G. H. Bokelman and W. S. Ryan, Jr., Analyses of Bright and Burley Tobacco Laminae and Stems, zur Tabakforschung International, 13 (1985) 29-36.

*Lancaster Labs, Lancaster, Pennsylvania

Temperature Dependence of Radical Formation from Hydroquinone and Catechol

Lavrent Khachatryan, Hiue Truong, Lacramioara Negureanu,
Randall Hall, and Barry Dellinger
Biodynamics Institute and Department of Chemistry, Louisiana State University
Baton Rouge, Louisiana

Hydroquinone and catechol derivatives are thought to be major molecular precursors for semiquinone radicals in the combustion of tobacco. However, the temperature dependence and characterization of radicals from the controlled thermal degradation of hydroquinone have not been reported in the literature.

We report the radical formation from the pyrolysis of hydroquinone and catechol from 200 to 1000 °C conditions. Radical formation is observed to increase with increasing temperature.

Molecular orbital a*b initio* density function calculations for semiquinone isomers and analogues demonstrate the effect of resonance stabilization on the structure of the radicals. Spin density calculations indicate that the semiquinone radical can exist both in the oxygen-centered and the carbon-centered structures of valence bond theory. Substitution effects the relative magnitude of the spin densities on each carbon or oxygen, but both structures still have significant contribution to the overall location of the unpaired electron.

A model of surface stabilization of these radicals is proposed that ties up potentially reactive sites through association with the surface. Once in biological systems, the semiquinones can be extracted from the surface to initiate biological chain reactions.

Development of Monitoring Techniques for Hydrogen Peroxide Related to Exposure to Cigarette Smoke

F. Yan, R. Jagannathan, G.D. Griffin, C. J. Brown, D. L. Stokes,
A. L. Wintenberg, and T. Vo-Dinh
Advanced Biomedical Science and Technology Group
Oak Ridge National Laboratory, Oak Ridge, Tennessee

In this work we describe the biosensing approaches that can be used to monitor hydrogen peroxide (H_2O_2) related to exposure to cigarette smoke. Hydrogen peroxide is a central oxygen metabolite, produced in several cellular compartments and the source of other reactive oxygen species (ROS) such as hydroxyl radical. We investigated several spectroscopic methods that can be used to sensitively detect H_2O_2 in aqueous samples. Emphasis is based upon the sensitivity as well as selectivity of the methods for analyzing H_2O_2 in complex samples. Research standard cigarettes are smoked on a five-channel smoking machine, and the gaseous phase is bubbled through water; the resulting H_2O_2 samples are collected with/without filtration of total particulate matter (TPM). The sensitivity of the detection methods is investigated. In this work, two indicators, 2'-7'-dichlorofloresc in and Amplex red reagent (a derivative of dihydrophenoxazine), are evaluated as probes for H_2O_2 detection using enzymatic fluorometric assays. In both cases, the amount of H_2O_2 increases gradually with time at room temperature, and approaches the maximum value over several hours. The kinetics of the production of H_2O_2 in the presence of total particular matter (TPM) is shown to be very different from that in the absence of TPM. The usefulness and potential of the spectroscopic techniques for monitoring of H_2O_2 in biological systems, especially in living cells, are discussed.

Effect of oxygen on the characteristics of Bright tobacco char

W. Z. Zhu, W. Geoffrey Chan, and Mohammad R. Hajaligol
Philip Morris USA, Richmond, Virginia

Hypothesis: The characteristics of Bright tobacco char can be dramatically affected by introducing small amount of oxygen during pyrolysis. By comparing tobacco chars prepared under both reducing and slightly oxidizing atmospheres using TG/MS, SEM, BET surface measurements, the effect of the oxygen addition can be delineated.

Results:

- TG/MS: Oxidative char exhibits significantly more weight loss than the nonoxidative char as they are heated to 1000°C in helium atmosphere. Although mass 18 comes off at comparable temperatures for both oxidative and nonoxidative chars, the amount released from the oxidative char is greater than from the nonoxidative char. Mass 44 comes off at much higher temperatures from oxidative char than nonoxidative char, as clearly shown by its evolution profile. Furthermore, remarkably greater amount of mass 44 is liberated from oxidative char than nonoxidative char. In contrast, more aromatic compounds are generated for chars prepared in the absence of oxygen.
- SEM: The vesicle formation indicating the onset of melting and evolution of volatile compounds during pyrolysis starts at lower temperature due to the introduction of oxygen. The degradation of major tobacco constituents such as cellulose and hemicellulose is made more extensive and severe in the presence of oxygen.
- BET surface: Oxidative char shows consistently larger surface area at each pyrolysis temperature than the nonoxidative char. It additionally displays more cumulative pore volume and broader pore size distribution; although exceptions are found for chars obtained at some pyrolysis temperatures.

Conclusions: Oxygen in the amount of 5% is shown to exercise marked effect on the tobacco char in terms of temperature and amount of mass released upon heating in helium, morphology, surface area and pore size distribution. Present results indicate that both the chemical and physical characteristics of tobacco char greatly depend on the pyrolysis condition.

Analytical Constituents Evaluation Laboratory: Development of an FT-IR Spectrometer – 5-Port Smoking Machine Instrument for Rapid Quantitative Analysis of Gas Phase Constituents in Cigarette Smoke

Susan Plunkett and David Self
Philip Morris USA, Richmond, Virginia

The Analytical Constituents Evaluation (ACE) Lab was formed to provide rapid, comprehensive analytical feedback on prototype samples. A number of methods were developed including the constituent classes carbonyls, volatile organic compounds (VOCs), a GC-MS method for volatile, semi-volatile, and high molecular weight organics, and an FT-IR method for low molecular weight gases.

A Midac FT-IR spectrometer was interfaced to a KC Automation 5-port linear smoking machine. Customization included the addition of 1/8" Teflon™ heated transfer lines, heated glass syringes with Teflon™ plungers, heated Cambridge filter pad holders, and software that controls both instruments and automates both data collection, processing, and presentation in Excel™ format. The gases measured quantitatively were: acetaldehyde, carbon dioxide, carbon monoxide, ethane, hydrogen cyanide, isoprene, and nitric oxide. Relative qualitative values for acetone, acrolein, 1,3-butadiene, carbonyl sulfide, ethylene, formaldehyde, methane, methanol, propylene, and water are also available. Method validation data include inter- and intra-day statistical process control charts for the 2R4F cigarette and an intra-laboratory 9 brand study spanning full-flavored to ultra-low delivery products. Instrument development, validation data, and sample data for low-CO delivery cigarettes will be discussed.

Analytical Constituents Evaluation Laboratory: Rapid Screening Methods for Smoke Constituents in Mainstream Smoke

C. B. Huang and David Self
Philip Morris USA, Richmond, Virginia

Analytical Constituents Evaluation (ACE) Laboratory has developed two rapid screening systems to analyze hand-made and machine-made prototype cigarettes with a quick turnaround time. One of the rapid screening systems is the puff-by-puff qualitative GC/MS method that (1) requires no sample preparation, such as solvent trapping or solvent extraction of Cambridge pad, (2) uses one cigarette per analysis for constituents in main stream smoke, and (3) monitors analytes in main stream smoke using a single puff or multiple puffs. Results are reported out as a percent reduction/increase compared to a control. The flexibility, sensitivity, feasibility and precision of the GC/MS system for analyses of volatile organics, PAHs, and flavor compounds in MS and data of interlab brand study and results from case studies, such menthol delivery and flavor capsule in SCoR cigarettes will be present. The other rapid screening method is a quantitative FT-IR gas phase system which consists of a Midac FT-IR spectrometer interfaced to a KC Automation 5-port linear smoking machine. Customization included the addition of 1/8" Teflon™ heated transfer lines, heated glass syringes with Teflon™ plungers, and software that controls both instruments and automates data collection, processing, and presentation in Excel™ format. The gases measured quantitatively were: acetaldehyde, carbon dioxide, carbon monoxide, ethane, hydrogen cyanide, isoprene, and nitric oxide. Relative qualitative values for acetone, acrolein, 1,3-butadiene, carbonyl sulfide, ethylene, formaldehyde, methane, methanol, propylene, and water compared to a control are also available. Method validation data include inter- and intra-day statistical process control charts for the 2R4F cigarette and an inter-laboratory 9 brand study spanning full-flavored to ultra-low delivery products. Instrument development, validation data, and sample data for low-CO delivery cigarettes will be discussed. Three validated test methods were implemented by ACE Lab to quantitate Volatile Organics (VOC's), PAHs, and Carbonyls in main stream smoke using GC/MS, LC/FLD, and LC/DAD. Interlab brand study data for VOC's, PAH's and Carbonyls from the ACE Lab, PTL and AMA are compared and presented. The Phenolic Method will be implemented in September 2003 and the TSNA method will be implemented by November 2003.

A Real-time GC/MS method for Puff by Puff Analysis of Whole Smoke

I. Skinner[1], D. S. Kellogg[1], H. Yu[1*], and Ric Brower[2]
[1]Philip Morris USA, Richmond, Virginia
[2]Shimadzu Scientific, Columbia, Maryland

We are in the final developmental stages of a unique GC/MS method designed to qualitatively analyze individual components of whole smoke on a real-time puff by puff basis. We are using a specially designed injection system jointly designed with Shimadzu Scientific, that allows sequential injection of each puff directly into the GC. The smoke, which is directly injected onto the column, can then be separated and subsequently identified using Mass Spectrometry. We have demonstrated that 7-puff resolution can be obtained for several classes of low molecular weight compounds such as isoprene, acetaldehyde and isovaleraldehyde, propene, 2-methyl furan, benzene and toluene, as well as semivolatile compounds such as limonene, menthol and nicotine.

*Lancaster Laboratories, Lancaster, Pennsylvania

Influence of Preheating Tobacco on the Yields of Smoke Products

Wei-Jun Zhang, Mohammad S. Rostami and Firooz Rasouli
Philip Morris USA, Richmond, Virginia

The vast majority of smoke products are generated by thermal decomposition and combustion of tobacco in a burning cigarette. Identifying the formation source and location of various smoke products in a burning cigarette will assist in developing techniques for reducing undesired compounds in smoke. In this work, we examined the effect of preheating tobacco at 110~270°C on the yields of gas vapor phases and PAHs in main stream smoke. We found that preheating tobacco at 270°C in air for 15 min leads to the reduction of TPM, NO and CO of 74%, 72% and 38%, respectively. The reductions of isoprene, methanol and acetaldehyde have the same trend as NO, with ~70% reduction at 270°C. Whereas CO_2, COS, HCN and acetylene are less sensitive to pre-heating as CO, with ~40% reduction at 270°C. The yields of ethylene, ethane and methane are basically not affected by pre-heating. Preheating the tobacco at 270°C results in ~50% increase in PAHs (phenanthrene, fluoranthene, pyrene and BaP).

Determination of Molecular Parameters for Quantitation of Non-HITRAN Molecules using Lead-Salt Tunable Diode Laser Infrared Spectroscopy

Charles N. Harward[1], Randall E. Baren, and Milton E. Parrish
Philip Morris USA, Richmond, Virginia

Hypothesis: To develop a reproducible and verifiable technique for generating a data file for constituents in cigarette smoke whose molecular parameters are not known and whose infrared spectra consist of large numbers of overlapping lines.

Results: A technique has been developed for the determination of a set of molecular parameters (line positions, line strengths, and air broadening coefficient) for the quantitation of non-HITRAN molecules using a dual channel lead-salt Tunable Diode Laser Absorption Spectroscopy (TDLAS) system that was developed for the quantitation of gaseous constituents in cigarette smoke. Several molecules of particular interest have populations of highly overlapping absorption lines in their spectra. Experiments were conducted that determined the line positions and line strengths for 1,3-butadiene and propylene for the first time. It was demonstrated that a sub-set of selected lines were sufficient to allow quantitation for intra-puff measurements.

Conclusions: The developed technique provides a way of estimating the molecular parameters for these overlapping absorption lines from quantitative reference spectra taken with the TDLAS at different pressures and concentrations for 1,3-Butadiene.

[1]Nottoway Scientific Consulting Corp., Nottoway, Virginia

Formation Mechanisms of Nitrogenous Char and NO During Biomass Oxidation

Hoongsun Im, Firooz Rasouli, Mohammad R. Hajaligol
Philip Morris USA, Richmond, Virginia

Hypothesis: The interaction between pectin and amino acids or proteins first produces nitrogen-containing char at a temperature below 350 °C either under pyrolysis or oxidative conditions. Then this char-N is further oxidized to produce NO. The mechanism of the formation of nitrogen-containing char can be confirmed by testing model compounds.

Results: Two char samples were prepared by heating biomass, such as peanut shell or tobacco, to 350 °C where the temperature was held for 30 min. One char was produced under pyrolysis conditions while the other one was produced under a partially oxidative condition (3% oxygen). NO formation has been observed from both types of char during oxidation at the high temperature range. The model system, the mixture of pectin and 10% proline, also shows the same behavior.
The chars prepared from the mixtures with cellulose under a similar condition did not produce NO. Elemental analysis of char produced at 250 °C shows that the nitrogen content in the char from the pectin mixture is much higher than that from the cellulose mixture.

Among lignocellulosic compounds, only pectin contains carboxylic acid functional groups in the structure. Amino acids have amine functional groups in the structure. It is conceivable from these facts to assume that the amine groups in amino acid and the carboxylate groups in pectin interact to fix nitrogen in the char. A few compounds with known structures were chosen; ploygalacturonic acid, a polymer with the subunit of pectin; chlorogenic acid, a phenolic compound with a saccharide unit; and, rutin, a phenolic compound with no saccharide unit. The first two compounds have the carboxylic acid functional group but rutin does not contain any acid group. The mixture of each acid and 10% proline produced NO at the high temperature range during the oxidation; but the mixture of rutin and 10% proline produced no NO at all.

Conclusion: The char formed around 350 °C during biomass combustion produces NO at the high temperature in the oxidative conditions. The results of model compounds studies confirm that the condensation reaction between the carboxylic acid functional groups in biomass and the amine functional groups in amino acids lead to the fixation of nitrogen in char. Then this char-N is oxidized further at the high temperature to produce NO.

The Role of Tobacco Solanesol in PAH Formation

Thomas E. McGrath, Gail Yoss, Jan B. Wooten and W. Geoffrey Chan
Philip Morris USA, Richmond, Virginia

Hypothesis: In understanding the formation mechanism of PAHs from tobacco, it is essential to pinpoint potential precursor pools, and given the complexity of the tobacco matrix, solvent extraction may be a tool we can use to estimate the contribution of component classes to smoke products. Although this approach has already been used in the past, the high temperatures used (>700 °C) have now been brought into question in light of our proposed lower temperature PAH formation mechanism. Does solanesol contribute to the overall PAH yield obtained from a burning cigarette?

Key Results:

- Solanesol occurs at levels as high as 4% of the dry weight of lamina and is therefore the most abundant tobacco terpenoid.
- Extraction of bright lamina with hexane, ethyl acetate, and ethanol removes increasing amounts of solanesol. Extraction with cold water increases/concentrates the amount of solanesol in the lamina. The extracted laminas were characterized by EA and NMR.
- Pyrolysis of the four solvent extracted laminas resulted in various amounts of BaP being formed. The yield of BaP could be correlated with the solanesol content of each extracted sample.
- Pyrolysis of solanesol at 600 °C in a tube furnace did not produce PAHs.
- The co-pyrolysis of cellulose with 10% w/w of solanesol at 600 °C yielded three times the amount of BaP formed from just cellulose alone.
- Solanesol decomposes at a higher temperature than cellulose – solanesol can still be observed in tobacco lamina that has been pyrolyzed to 350 °C.

Conclusions: There is a direct correlation between the amount of solanesol extracted/concentrated and the decrease/increase in BaP yields. It is proposed that solanesol decomposition in the presence of cellulose or tobacco low temperature char gives rise to the formation of PAHs.

Conclusions Regarding the Product: The selective reduction/removal of solanesol from bright and burley tobacco lamina may potentially reduce the yields of PAHs from a lit end cigarette.

Phenolic Compound Formation from Tobacco and Tobacco Components

Gayle M. Powers, **Raquel M. Olegario**, Thomas E. McGrath, and W. Geoffrey Chan
Philip Morris USA, Richmond, Virginia

Hypothesis: Phenolic compounds can be accurately measured by HPLC-fluorescence using a non-aqueous extraction solvent.

The goal of the present work was to develop a versatile method where phenolic compounds and polycyclic aromatic hydrocarbons (PAH) could be quantified in the same extraction solution.

Key Results:

- Methanol is used as extraction solvent.
- The same methanol extract can be used to analyze PAH by CG/MS and phenolic compounds by HPLC-fluorescence.
- 12 phenolic compounds and 16 PAH can be quantified.
- The method is applicable to cigarette mainstream total particulate matter (MS TPM) and pyrolysis tar.
- The method is also applicable to puff per puff analysis of MS cigarette smoke.
- The sample preparation is simple.
- For phenolic compounds present in MS smoke of reference cigarettes the results obtained by this new method are in good agreement with those obtained by aqueous extraction of TPM.

Conclusions: We have developed a fast and versatile research analytical method to quantify phenolic compounds in MS cigarette smoke and pyrolysis tar.

Conclusions Regarding the Product: Such analytical tool can be used to support research and the development of potentially reduced exposure products.

A Tunable Laser System for Single Particle Mass Spectrometry

Ramkuber Yadav, Joseph Banyasz, Mohammad Hajaligol
Philip Morris USA, Richmond, Virginia

Resonance enhanced multi-photon ionization (REMPI) – time of flight mass spectrometry is a sensitive and selective technique, well suited to identify species such as organic molecules present in complex gas mixtures. Traditionally REMPI is used for gas phase studies; here we describe the applicability of this methodology to particulate phase studies. A pulsed optical parametric oscillator (OPO) laser system equipped with frequency doubling option was added to our existing aerosol time of flight mass spectrometer (ATOFMS). In addition to the OPO, we also have the capability to generate various harmonics including an output of 213 nm wavelength from the 5^{th} harmonic of Nd:Yag. From stability and beam quality considerations, these OPO systems have been designed to operate at a fixed frequency, whereas in single particle mass spectrometry the particles arrive in a random fashion at the laser ionization spot. Thus, in order to successfully ionize the particle, it is imperative that the laser pulse arrives at the ionization spot synchronously with the particle. In the present work, we describe the incorporation of an OPO based laser system into an ATOFMS system. The applicability of this system is demonstrated by tuning the laser wavelength to selectively ionize a single component in a multi-component mixture.

Reentrainment of Submicron Solid Particles from Inside Cylindrical Surfaces

Ramin Mortazavi[1], Timothy Cameron[1], James McLeskey[1], Mohammad Hajaligol[2]
[1]Department of Mechanical Engineering, Virginia Commonwealth University, Richmond, Virginia
[2]Philip Morris USA, Richmond, Virginia

Solid nanoparticles may be used as catalysts in cigarettes to reduce harmful combustion and pyrolysis products. Concerns exist that nanoparticles may themselves be entrained in the mainstream smoke and have undesirable effects. In this work the entrainment of submicron solid particles from the inside of cylindrical surfaces of glass and metallic materials are measured and the results are compared to available models and experimental data. SEM images are used to show the influence of roughness of substrate and particle in reentrainment. It is shown that entrained particles are of the same size used in deposition and its concentration decays in the form of $C = at^n$.

Performance of an Aerosol Sampling and Dilution system

Ali Rostami, Steven Larson, and Sue Wrenn
Philip Morris USA, Richmond, Virginia

Hypothesis: The loss of aerosols or nanoparticles in the tubing and fittings from the sampling point to the aerosol measurement system is a major problem that affects the accuracy of aerosol characterization instruments. We have designed and tested the performance of an aerosol sampling and diluting system that can provide a dilution ratio of over 1000 in a continuous operation. There is no need for a valve in the sampling line and the total length of the sampling line may be as small as 30 cm.

Diluter design: The system consists of a stationary and a moving tubes as well as a replaceable capillary all aligned on the same axis. The truncated cone ends of the two tubes make a male and female match producing an annular flow passage for the dilution air. The dilution ratio can be adjusted by the linear motion of the moving tube along the axis as well as by using capillary tubes with different sizes and lengths. The sample flow rate is measured by the vacuum in the stationary tube, which is linearly related to the laminar flow rate in the capillary.

Results: A 200 mm long capillary tube with an internal diameter of 760 μm was used for preliminary evaluation of the system. The vacuum in the fixed tube (capillary outlet) was changed from 1.4 to 38 cm H_2O, with the corresponding sample flow rate of 0.018 to 0.445 LPM. With the total air flow rate remained at 25 LPM during the test, the highest value of the dilution ratio achieved was 25/0.018 = 1388. It is evident that the length of the capillary tube and the sample gas velocity in the tube play important roles on the diffusion loss. This will be the criteria for choosing the right capillary internal diameter. Tests are being carried out to determine the right combinations of capillary ID and length for minimum particle losses.

A Parametric Study of Transport of Aerosol Particles in a Heterogeneous Shredded Porous Media

M.S. Saidi, **K. Shafer**, P. Lipowicz,
Philip Morris USA, Richmond, Virginia

The size distribution and the total number of aerosols passing through a porous media is changed due to coagulation and deposition. The change in aerosol number density and the rate of aerosols absorbed in the media not only depends on the bed geometry, but also depends on bed packing density and flow temperature and velocity field.

Here the model developed for simulating the transport of aerosol particles in a shredded porous media is applied to study the effect of a bed of cylindrical shape with 8 mm diameter and 70 mm length on passing aerosol with a log-normal distribution.

The numerical calculation shows that aerosols mean diameter increases while passing through the media. The rate of absorption increases with increasing the total number of incoming aerosols. The mean diameter of absorbed aerosol particles increases with increasing the total number of incoming aerosols. This is due to the fact that higher number concentration leads to higher rate of coagulation and thus larger mean diameter. The calculation shows that aerosols with smaller initial mean diameter are absorbed more due to the fact that Brownian absorption is more effective for smaller sizes. Increasing the packing density increases the rate of deposition and also the change in size distribution is more pronounced. Decreasing the inlet flow velocity increases the residence time and causes more coagulation and deposition. Increasing the bed temperature increases the rate of deposition. The effect of bed length on the transport of smoke aerosols mean diameter is calculated and compared with experimental results. One set of experimental data is derived using the extinction method and the other one using CPC. Our numerical results are more closer to the extinction method data because in this method we don't have unwanted mean diameter increase due to aging effect.

Correlation of Gas Phase Products with Char Composition Resulting from Maillard Chemistry

Bob Evans, Thomas Sherow, Karl Andreason, Mike Looker,
Mark Nimlos and Luc Moens
National Renewable Energy Laboratory
Golden, Colorado

Hypothesis: Correlation of the solid phase and gas phase products from Maillard chemistry are important for understanding how this chemistry affects the maturation of char in a cigarette and the emissions of PAHs and other volatiles. We have measured the gas phase products from Maillard chemistry using Molecular Beam Mass Spectrometry (MBMS) and have analyzed the remaining char using FTIR and elemental composition. In addition, we have measured the weight loss of the solid material during temperature ramps. In our experiments we have also studied the effects of sequential temperature ramps on the chemistry and maturation of the char. We mix amino acids with glucose in a matrix containing cellulose and pectin and pyrolyzed these in flowing hot helium. These are important constituents of biomass which produce representative yields of char and enable the study of solid phase reactions.

Results: There are several interesting observations regarding the evolution of products and the transformation of the solid material.

- At low temperatures the gas phase products are dominated by water loss. In the solid phase these emissions are accompanied by a conversion of hydroxyl (OH) groups into carbonyl (C=O).
- Higher temperatures result in the emissions of more carbonaceous species and in the growth of aromatic groups in the solid. The stoichiometry of the gas phase product is such that aromatic or substituted aromatic compounds are likely in this mixture.
- The types of gas phase products from pyrolysis of the char depend upon the thermal history of the solid.
- The nitrogen content of the solids increases with reaction severity.

Conclusions: MBMS measurement of gas phase products from pyrolysis of mixtures of carbohydrates and amino acids and analysis of the remaining solid allows the identification of important chemical transformations in the maturing of char. In addition, the effect of char maturation processes on gas phase emissions can be modeled.

Synthesis and Characterization of Nanocrystalline Cu/CeO_2 catalyst for CO Oxidation by Laser Vaporization and Controlled Condensation Method

R. S. Sundar, S. Deevi and D. Miser
Philip Morris USA, Richmond, Virginia

Hypothesis: Laser ablation of materials results in materials with non-equilibrium structures and high concentration of structural defects. Defects play an important role in catalytic activity. We explore preparation of $Cu\text{-}CeO_2$ catalysts by Laser Vaporization and Controlled Condensation to promote CO oxidation reaction.

Results: Ceria supported copper (2-70 wt.% Cu) catalysts have been synthesized by laser vaporization and controlled condensation method and characterized by X-ray diffraction (XRD), transmission electron microscopy (TEM) and energy dispersive x-ray analysis (EDAX). The catalytic activity of the nanopowders for CO oxidation reaction was tested in a fixed bed flow tube reactor in a $Ar\text{-}20\%O_2\text{-}4\%CO$ mixture. Irrespective of the copper content, the catalytic activity of the nanopowders is similar in the initial run and the catalytic activity improves (i.e. decrease in light-off temperature) during the second run. The lowest light off temperature during the second run is recorded when the copper content is between 20-40%. TEM and EDAX results reveal that in the as-prepared sample, ceria is present as CeO_2 and CeO_{2-x} and copper exists in solid solution as well as surface Cu_2O layer over the CeO_{2-x} particles. The sample examined after CO test contains additional fine CuO crystals within the CeO_2. Our TEM results suggest that the shift in light-off temperature during the second run is due to a synergistic interaction between newly formed CuO crystals with the CeO_2 matrix.

Conclusions: Active CeO_2-Cu catalysts are prepared by LVCC method. Though we have observed the non-equilibrium (reduced form of CeO_2) in the laser ablated material, the catalytic activity is mainly due to synergistic interaction between the finely dispersed CuO and CeO_2.

Commercially Available color Pigments as Potential Candidates for CO Oxidation Catalyst

S. Gedevanishvili, S. PalDey, F. Rasouli
Philip Morris USA, Richmond, Virginia

Commercially available pigments containing a range of metal oxides were tested for CO oxidation ability. Black- 444 pigment of Shepherd Color Company performed the best. XRD analysis of Black 444 powder showed existence of $Cu_{1.5}Mn_{1.5}O_4$ spinel structure in mixed Fe_2O_3 and Mn_3O_4 oxide base. The mixed oxide is quite stable at high temperatures and found to be capable of providing oxygen for CO oxidation even in oxygen deficient conditions which generally prevails in a burning cigarette. Application of Black 444 in cigarette filler led to removal of a significant amount of CO. Experimental evidence showed that dispersion of catalyst on inert support of Al_2O_3 played a critical role for the catalyst activity in cigarette applications. Based on reducibility tests and characterization by XRD a synergestic effect between individual constituent metal oxides is proposed. Mixed oxides of transition metals thus provide an alternative to expensive noble metal containing catalysts for cigarette applications for removing toxic CO gas.

Effect of Changes in Crystalline Phases and Microstructure on the CO Oxidation Activity of Pd/ZnO-based Catalysts

Yezdi B. Pithawalla, Rangaraj S. Sundar, Jan A. Lipscomb and Sarojini Deevi
Philip Morris USA, Richmond, Virginia

Hypothesis: Fundamental understanding of changes in the crystalline phases and microstructure during catalytic testing can help better understand activation and deactivation of the catalyst.

Results: The freshly prepared catalyst formed by the co-precipitation of $PdCl_2$ & $ZnCl_2$ has a BET surface area of 46 m^2/g and is found to contain $Zn_5(OH)_8Cl_2.H_2O$ and ZnO by FTIR and XRD analysis. The presence of Pd in the freshly prepared catalyst is verified by TEM, EDX and XRF analysis. During the first run of testing for catalytic activity an initial high activity towards CO oxidation ($CO+1/2\ O_2 \rightarrow CO_2$) is observed at low temperatures followed by a decrease in activity at intermediate temperatures and regaining of activity at higher temperatures. Catalytic activity for all subsequent runs is found to be stable. XRD, FTIR, TEM, XRF, EDX and HR-TGA results will be used to explain changes in the crystalline phases and microstructure of the catalyst during testing for catalytic activity. It will be demonstrated how chloride poisoning is responsible for the decrease in activity at intermediate temperatures and removal of chloride ions from the catalyst at higher temperatures leads to the regeneration of catalytic activity with the formation of a stable PdO/ZnO catalyst. The effects of increasing the number of active sites by increasing the surface area and decreasing the number of active sites by calcination on the CO oxidation activity of the freshly prepared catalyst will be discussed. Results of catalytic activity of the PdO/ZnO catalyst towards oxidation of CO present in a gaseous stream generated from mainstream cigarette smoke will also be presented.

Conclusions: Activation & deactivation of a catalyst can be directly correlated to changes in its crystalline phases and microstructure both of which can occur during catalytic testing. Understanding these changes at a fundamental level will help design more efficient and selective catalyst.

Thermal Reaction of Catechol over Nano-Particle Iron Oxide and Quartz

Eun-Jae Shin, Mohammad R. Hajaligol, W. Geoffrey Chan and Firooz Rasouli
Philip Morris USA, Richmond, Virginia

Hypothesis: Catechol can be converted to more desirable products with lower energy barrier in the presence of nano-particle iron oxide.

Results:

- The nano-particle iron oxide lowered the temperature of a given conversion by about 200°C, compared with that over quartz.
- Catechol cracking products were classified into four groups by using factor analysis: primary, secondary I, secondary II and tertiary products.
- Higher catechol concentrations suppressed conversion without significant changes in product distribution.
- Oxygen concentration had insignificant effects on conversion and product distribution.
- Temperature affected conversion and product distribution significantly over both quartz and iron oxide/quartz:
  - Quartz: T ↑ → Secondary II Products ↑
  - Iron Oxide/Quartz: T ↑ → Tertiary Products ↑
- The quartz surface defects led to an unexpected conversion and limited reactions of catechol.
- The activation energy over iron oxide was reduced by factor of 2.

Conclusions:

- Catechol becomes very unstable and converted to more desirable products over iron oxide.
- Lower activation energy in the presence of iron oxide indicates strong catalytic effect.

Porosity Development and Graphitization of Non-Graphitizing Carbons Below 2000 °C

Donald Miser[1*], Diane Gee[1, 2], Gary Wnek[2], Mark Zhuang[1], Peter Lipowicz[1], and John Layman[1, 2]
[1]Philip Morris USA, Richmond, Virginia
[2]Department of Chemical Engineering, Virginia Commonwealth University, Richmond, Virginia

Hypothesis: Carbon fibers formed from phenolic and polyacrylonitrile (PAN) resins are referred to as non-graphitizing carbons, while mesophase pitch will produce graphite at 3000 °C. Non-graphitizing carbons are purported to consist of a tangle of graphene sheets, *i.e.* each sheet approximates the two dimensional structure of graphite but with an absence of a three dimensional structure. Carbonized phenolic resin fibers, however, have been shown to contain graphitic layers at the fiber perimeters, as well as decreasing diameters of ultramicropores and supermicropores in the temperature range up to 1400 °C by BET. However, above this temperature the ultramicropores appear to disappear. It is hypothesized that electrospinning premotes graphite development by alignment of the precursors and as temperature is increased all of the carbon contracts and approaches a graphite structure. As the graphene sheets contract and approach an interlayer thickness of graphite, the size of the ultramicropores, which may represent these spaces, also decreases. Continued heating would result in the predominant formation of graphite with an interlayer spacing of 3.34 Å. However, pores below about 4 Å would remain undetected by BET, thus HRTEM was employed to study this transition.

Results: X-ray diffraction showed broad intensities representing averaged decreasing d-spacing with increasing temperature, supporting the hypothesis. HRTEM of the carbon, similarly showed a decrease in the interlayer d-spacing with increasing temperature. In addition, there seemed to be an increase in the number of graphene sheets associated with the graphite-like packets. Quantities of true graphite were found at temperatures as low as 1600 °C in phenolics. PAN, which was more sluggish to would transform by the addition of transmission metal catalysts at lower temperatures. Graphite readily formed by 1200 °C for iron catalyzed PAN. Increasing amounts of this graphite combined with decreasing volume of graphene sheet material would result in an apparent decrease in the observed d-spacing by X-ray diffraction. Furthermore, the presence of {10.1} and 10.0} intensities in the HRTEM images indicated that both R`3 and 2H graphite have formed, sometimes within the same crystal.

Conclusions: Packets of graphene sheets form from carbonized fibers. Inter particle porosity contributes to supermicropores measured by BET methods. Interplanar spacing constitutes the ultramicropores. The interplanar porosity decreases below the detection limit of the BET method as crystalline graphite is approached. Electrospinning promotes this graphitization,, especially at fiber perimeters where shear forces may be important. Thus the porosity measured

of electrospun fibers is a combination of that promoted by electrospinning and that induced by temperature of non-electrospun phenolics.

A Comparison of Menthol Delivery from Two Menthol Release Agents and their Thermal Properties

Kathryne Esperdy
Philip Morris USA, Richmond, Virginia

Hypothesis: Menthol precursors, such as menthyl itaconates and menthyl carbonates, have been studied since the late 1970's as a way to deliver menthol in a cigarette. The virtue of these compounds was to prevent menthol migration into the filter and packaging material since the precursors release menthol only at the moment of pyrolysis. Beta L-menthyl potassium itaconate and 1-D-mannitol, L-menthyl carbonate are two selected compounds from this body of research that are currently being reinvestigated as release agents for menthol delivery in test cigarettes with modified carbon filters. The menthyl -itaconate and -carbonate compounds can be added to tobacco filler in test cigarettes in one of three ways: 1) directly as a powder, 2) sprayed on as an ethanol or water solution and dried, and 3) as ethanol or water liquid cores in microcapsules. Microcapsules are being investigated as a menthol delivery vehicle because the menthol precursor in liquid form may enhance the cooling effect of the menthol released and aid in delivering more menthol to mainstream smoke, especially if water is present.

Results: The data for menthol in mainstream smoke for both release agents is comparable to the level of menthol in smoke from other menthol delivery systems, such as menthol in starch microcapsules and menthol in polyvinyl acetate film. In filler loaded with 1-D-mannitol, L-menthyl carbonate, ~17 mg of menthol could theoretically be released in each test cigarette. An average of 0.4 mg menthol was delivered when the modified carbon filter was in place, and in control cigarettes that contain no carbon filters, 0.8 mg of menthol was delivered. Applying the carbonate precursor as a liquid and then drying the filler delivered more menthol than pyrolyzing it as a dry powder in the tobacco filler. The sodium and potassium salts of menthyl itaconate produced 0.1 mg and 0.2 mg of menthol per cigarette, respectively, about half as much as the control cigarettes for this test series. The theoretical level of menthol possible for these test sets was ~ 17 mg/ cigarette and the itaconates were injected onto the filler in a water solution and allowed to dry.

Conclusions: Thermal and pyrolytic properties for both types of menthol precursors show that the 1-D-mannitol, L-menthyl carbonate is a better release agent because of low volatility, low residue and very low levels of by-products. In contrast, the levels of menthol delivered from the –menthyl itaconates are low due to high amounts of menthene and itaconic anhydride produced upon pyrolysis at temperatures greater than 400 ^{o}C. Releasing menthol from a microcapsule appears to give the highest delivery and seems to be a superior method to using the release agents.